Palaeogeography, Palaeoclimatology, Palaeoecology 542 (2020) 109581

Contents lists available at ScienceDirect

Palaeogeography, Palaeoclimatology, Palaeoecology

journal homepage: www.elsevier.com/locate/palaeo

Lacustrine record of high magnitude flood events and climate variability during mid to late Holocene in the semiarid alluvial plains, western India

Alpa Sridhar[a,*], Biswajeet Thakur[b], Nathani Basavaiah[c], Priyanka Seth[b], Pooja Tiwari[b], L.S. Chamyal[a]

[a] Department of Geology, The M. S. University of Baroda, Vadodara 390002, India
[b] Birbal Sahani Institute of Palaeosciences, 53, University Road, Lucknow 226007, India
[c] Indian Institute of Geomagnetism, Kalamboli, New Panvel, Navi Mumbai 410218, India

ARTICLE INFO

Keywords:
Palaeofloods
Lacustrine sediments
Mineral magnetics
Palynofacies
Southwest monsoon

ABSTRACT

Long-term data on flooding events are necessary for understanding the flood frequency and magnitude variations, but the available instrumental records span only a few decades. Recently, lake sediment sequences have emerged as a relatively untapped archive for high-magnitude floods over longer timescales. In the present study, multi-proxy data from a lacustrine sequence at Timbi in the Dhadhar river basin were analysed to determine high magnitude floods in this semi-arid region of western India in response to southwest monsoon variability. The results indicate the occurrence of discreet high magnitude flood events and depositional phases corresponding to different climatic conditions during the mid to late Holocene. Three large flash floods between 4830 and 2730 cal yr B.P. (Phase-I) have been identified as coeval with flood events from fluvial archives and correlated to the widespread period of aridity and weak monsoon recorded in the lakes of north western India. A shift in the depositional environment from fluvial to lacustrine occurred around 2730 cal yr B.P. as inferred from an abrupt change in the sediment character and palynofacies caused by high intensity flash floods and high sediment influx. Phase II (2730–1730 cal yr B.P.) was marked by periodic erosion and deposition in the catchment and sediment influx during pulses of higher precipitation as evident in the dominance of *Glomus* sp. and *Alternaria* sp., and relatively low values in concentration-related magnetic parameters and S-Ratio. A high magnitude flood event occurred at 1770 cal yr B.P. towards the end of phase II. During phase III (1730–880 cal yr B.P.) the monsoon was enhanced and climate was warmer as suggested by low χfd%, SIRM/χ, S-Ratio, higher Ba/Sr ratio and presence of aquatic palynomorphs. A high percentage of structured Organic Matter (OM), low fungal remains and increased Ba/Sr ratios between 880 and 360 cal yr B.P. indicate higher lake waters and better monsoon condition during phase IV. The phase V (360–0 cal yr B.P.) corresponds to lake level lowering, soil formation and eutrophication. The Timbi lake sediments demonstrate the potential for lakes in semi-arid alluvial plains of western India to preserve proxy flood records providing additional archives for generating long-term datasets. The flood record generated substantiates palaeoflood data from the fluvial archive suggestive of regional-scale southwest monsoon variability. Low frequency-high magnitude floods occurred during arid periods and low magnitude-high frequency events during relatively strengthened monsoon and thus have implication for linking the palaeoflood events to the southwest monsoon intensity in the semi-arid continental regions.

1. Introduction

Floods are the most common natural hazards that cause widespread destruction, necessitating a comprehensive understanding about their future trends. Long-duration datasets of flood occurrence are necessary to study the flood frequency and magnitude variations. However, the instrumental data available are very short. Therefore, information on past floods are derived from archives such as slack water sediments, coarse clasts, erosional landforms and high-water marks along bedrock channels (Baker, 1987). In alluvial regions the highest magnitude floods are captured as discrete layers of silt and sand in overbank sequences and are preserved in incised, abandoned channels and flood basins (Sridhar, 2007a; Jones et al., 2012; Leigh, 2018). Lakes also form promising repositories for clastic material eroded from catchment slopes and floodplains (Oldfield, 2005) and hence lacustrine sequences have been increasingly studied during the last two decades as recorders

* Corresponding author.
E-mail address: alpasridhar@rediffmail.com (A. Sridhar).

https://doi.org/10.1016/j.palaeo.2019.109581
Received 2 April 2019; Received in revised form 23 December 2019; Accepted 23 December 2019
Available online 09 January 2020

of past floods (Wilhelm et al., 2012). Floods erode and transport large amounts of material from the lake catchment and generate the sediment-laden flows that deposit the mostly detrital material forming flood layers (Wilhelm et al., 2015). Such layers are preserved in undisturbed areas of the lake and stacked in sediment sequences, providing a great potential to reconstruct long and continuous flood series which may be missed in a fluvial sequence (Gilli et al., 2013). Across the globe, high-resolution lake sediment palaeoflood records have been generated in the last two decades based on multi proxy analysis of sediment layers in upper river catchments (Bøe et al., 2006; Page et al., 2010; Wilhelm et al., 2012; Wirth et al., 2013; Schlolaut et al., 2014; Bird et al., 2016) as well as lower river reaches (Li et al., 2013; Reinwarth et al., 2013; Toonen et al., 2015; Munoz et al., 2018) but none from the Indian subcontinent.

In India, the lacustrine records have been investigated to address the climatic variations resulting in the spells of dry, wet, cold, and warm conditions over the subcontinent during the Holocene using pollens, phytoliths, oxygen isotope ratios and mineral magnetics (Enzel et al., 1999; Basavaiah et al., 2004; Phartiyal et al., 2005; Achyuthan et al., 2007; Nair et al., 2010; Dixit et al., 2014; Prasad et al., 2014a; Prasad et al., 2014b; Mishra et al., 2015; Raj et al., 2015). However, lake sediment records also preserve signatures of river floods at an event scale and can be interpreted in terms of abrupt change in deposition environments (Bronstert, 2003), which is the focus of the present study.

The river hydrology and flooding in the semi-arid alluvial plains of western India are governed by the southwest monsoon variability (Sridhar and Chamyal, 2018). These alluvial archives and slack water deposits in particular, have been extensively explored in the river basins for reconstruction of Holocene flooding history and climatic variability (Ely et al., 1996; Kale, 1999; Kale et al., 2003; Sridhar, 2007a, 2007b; Sridhar et al., 2014, 2015, 2016) but the records are fragmentary. The climatic and tectonic changes during the late Pleistocene-Holocene time period led to avulsion in the rivers forming palaeochannels, lakes and ponds (Raj, 2004; Juyal et al., 2006). These features in turn have provided archives for palaeoflood studies since the flood events are discernible as layers of detrital material within the authigenic lacustrine sediments (Wirth et al., 2013).

The primary objective of this study was to demarcate the layers of past flood events within the sediment archive in a lake basin in the alluvial plains of western India. Data on palynofacies, grain size, mineral magnetics, major elements and chronology were generated on the lacustrine sediment succession as proxy records of flood history spanning the past 5000 years. The multiproxy measurements showed a strong relationship with the sediment stratigraphy and are expected to enrich dataset of flood events in a sediment sequence from Indian lakes. Additionally, the role of southwest (SW) monsoon variability in the occurrence of flood events in the semiarid alluvial plains during the late Holocene was assessed.

2. Regional setting and the study site

The semi-arid plains of western India, more commonly known as the Gujarat Alluvial Plains, form the central part of the Gujarat State, western India. The plains extend for ~33,000 sq. km, fringing the Thar Desert margin to the North, the Eastern Hill ranges to the east, the Arabian Sea to the west and Sahyadris to the south (Fig. 1). These plains have formed owing to extensive sedimentation during the Pleistocene and are drained by numerous west flowing rivers such as the Sabarmati, Mahi, Dhadhar, Narmada and Tapi (Merh and Chamyal, 1997). The river valleys were formed during the early-Holocene enhanced monsoon conditions (Gupta et al., 1999). Since then, the factors of physiography, lithology, tectonics and climate have controlled the geomorphology of these river basins. Maurya et al. (2000) have described three lateral surfaces viz. the valley-fill terraces, the ravine surface and the alluvial plain surface which form the geomorphic ensemble in the region. The Dhadhar River originates from the Pavagarh hill (Fig. 1B), flows through the alluvial plains and merges into the Arabian Sea. The upland reach of the basin comprises the metamorphic rocks of Champaner Group belonging to the Aravalli Supergroup (Fig. 1B). Deccan Trap Basalts occur at the subsurface and are seen exposed as isolated hills. The alluvial and estuarine part of the basin occupies a part of the Cambay graben (Mathur et al., 1968) and comprises a basaltic basement overlain by thick (up to 500 m) Quaternary sediment sequences. The Dhadhar River has incised these sediments forming ravines (Fig. 1C) and the upper 18–20 m is seen exposed along the channel (Raj, 2004). A good number of lakes/ponds occurring in the alluvial plains (Fig. 1C) show thick fluvial record overlain by laminated lacustrine clays (Raj, 2004).

The Timbi lake is located in the Dhadhar River Basin (22°19′ N; 73°17′ E), has an area of ~3.5 sq. km and a catchment of about 15 sq. km (Fig. 1D). The lake is situated within the alluvial plain area and has a catchment in the pediment zone comprising thin veneer of Quaternary deposits and the sediment input is mainly from the Precambrian rocks of Champaner group and the Deccan volcanic basalts exposed to the east and northeast of the lake.

The lake is in the semi-arid climatic region of western India within the Core Monsoon Zone (CMZ) (inset Fig. 1). The climate of the region is sub-tropical with moderate humidity and average annual rainfall of 930 mm, but infrequent torrential rains cause flooding in the river. The land use in the catchment area of the lake is primarily agriculture barring the ravine areas seen as open scrubs.

2.1. Lithostratigraphy

The study is based on the observations and analysis of the sediment succession exposed by trenching at the fringe of the Timbi Lake (Fig. 1B). Continuous sampling was done from the section (4.2 m) in the lakebed at the inflow end so that maximum number of sediment pulses in the lake can be picked. A total of 42 sediment samples were collected from the main sequence at 5 cm resolution (BK 3 - BK 44), 4 samples from the weathered bedrock at 30 cm interval (BK 45 - BK 48) and 6 samples from the topsoil horizon at 20 cm interval (BK 2 -BK 1d).

The sediment succession of the Timbi Lake comprises five zones as classified based on the physical and stratigraphic character of the sediments (Fig. 2A). The topmost zone (zone V; 0–90 cm depth; BK 1d – BK 2) comprises pedogenised organic rich sediments, predominantly clay and silt (~40% each; Figs. 2A and 3). The underlying zone IV (90–185 cm; BK 3 - BK 21) is 95 cm thick and shows a significant increase in the sand (upto 70%), a decrease in clay (20%) and massive silt (10%) contents as compared to zone V (Figs. 2B and 3). Zone III (185–265 cm; BK 22 - BK 36), 80 cm thick comprises laminated intercalated silt and clayey silt horizons (Fig. 2A, C). A decrease in the sand content (~55%) and increase in the clay and silt content (20–25%) than zone IV is observed (Fig. 3). Six events of silt deposition can be demarcated, each followed by a thin (about 2 cm) organic rich clay layers. Zone II (265–305 cm; BK 37-BK 44) is distinctively different in character from the overlying zones. The sediments are loose, coarse and show planar cross stratifications (Fig. 2). The sediment grain size is predominantly coarse sand to fine gravel size with low content of silt (< 5%; Fig. 3). The bottom most zone I (305–425 cm depth; BK 45 - BK 48) comprises highly weathered basalt. The contact between the zone I and II is an erosional one, very sharp and distinct (Fig. 2B).

3. Analytical methods

Data on sediment grain size, palynofacies, major element concentration and mineral magnetic properties were generated to demarcate the flood events and to infer the palaeoenvironmental changes the area has undergone during the late Holocene.

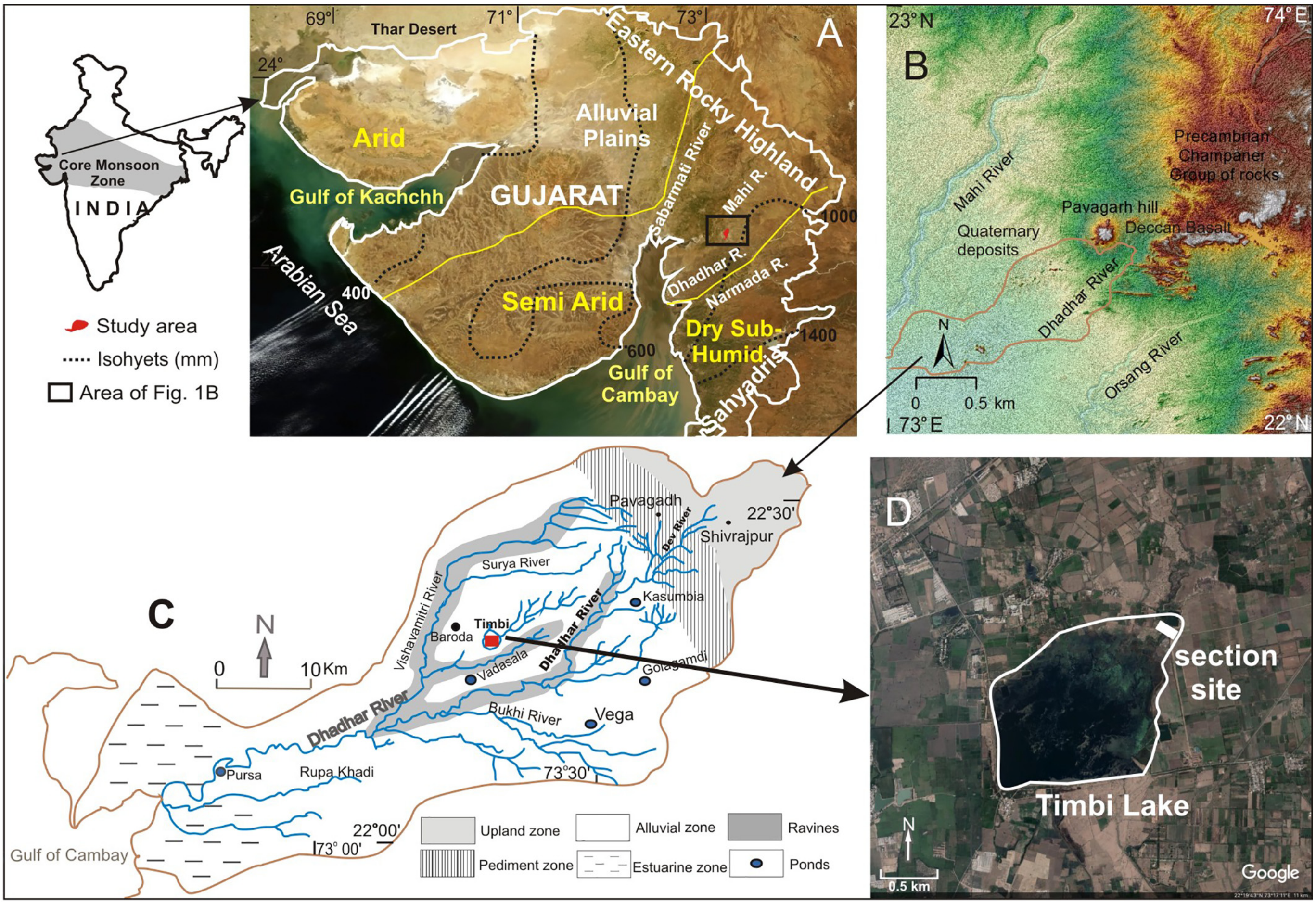

Fig. 1. A. Map showing the location of the study area, major physiographic features, climatic zones and isohyets in Gujarat. The box marked represents the area of Fig. 1B. Inset picture shows the core monsoon zone (CMZ) in India. B. 30 m DEM of the region around the Timbi Lake showing the general topographic features and the major rivers. C. Drainage of the Dhadhar River basin with marked geomorphic zones and major ponds/lakes (Raj, 2004). D. Google earth image of the Timbi Lake showing the present-day set-up and land use pattern. The artificial bund was built in the year 1952–1953 for irrigating the wide spread agricultural land.

3.1. Grain size analysis

To analyse the grain size distributions 48 sediment samples (BK 1d - BK 44) were pre-treated with hydrogen peroxide to eliminate Organic Matter (OM) and then oven dried at the Department of Geology, The M. S. University of Baroda, India. Around 100 g of sample was taken and subjected to sieving as per the standard procedure (Folk, 1968). The various size fractions obtained were weighed. The fraction < 63 µm was further treated with sodium hexametaphosphate solution overnight for deflocculation. The silt - clay fraction was analysed using Sedigraph and results noted (Fig. 3). The data were processed using Gradistat software for statistical parameters (Blott and Pye, 2001) of mean size, sorting, skewness and kurtosis (Fig. 3).

3.2. Palynofacies analysis

Palynofacies has been defined as a set of distinctive assemblages of various types of sedimentary organic matter (SOM) derived from sediments after the dissolution of carbonate and silicates (Combaz, 1964; Powell et al., 1990; Traverse, 1994; Tyson, 1995). The study of the palynofacies gained importance with an approach to define palaeoenvironmental reconstructions in the field of palynology to establish depositional settings (Pocknall and Beggs, 1990; Roncaglia, 2004; Sebag et al., 2006). Palynofacies has now been identified as a robust proxy for multi-dimensional studies like climate change, hydrodynamic conditions, oxic-anoxic environments, runoff related processes, proximal-distal trends, palaeoenvironments and archaeological studies, both in continental and marine records (Tyson and Follows, 2000; Hoaen, 2000; Closas et al., 2005; Zobaa et al., 2011; Carvalho et al., 2013; Mueller et al., 2014; Aggarwal et al., 2017). Initially the palynofacies approach was developed for pre-Quaternary studies due to their importance to petroleum exploration (Traverse, 1994; Tyson, 1995) for kerogen characterization. However, in recent few decades the application of palynofacies has broadened and now it has become a major proxy for Quaternary depositional environments (Roncaglia, 2004; Sebag et al., 2006; Thakur et al., 2019).

The major focus in the palynofacies study is the quantitative characterization of various phytoclasts, palynomorphs, zoomorphs, algal/fungal remains and amorphous OM (AOM) to establish the hydrographic regime and process driven changes in the study area. The details of the palynofacies components recorded in the present study are given in Appendix 1. The phytoclasts includes brown degraded OM, i.e. partially degraded plant remains; structured organic matter such as cuticles, wood and tracheid (Traverse, 1994; Tyson, 1995; Batten, 1996; Roncaglia, 2004); opaque phytoclasts, i.e. black debris that refers to oxidized brownish – black to black woody tissues, including charcoal. The palynomorphs comprises of various microfossils like pollen/spore and dinocysts while the zoomorphs encompasses animal vestiges and shell carapaces; the AOM is used to define particulate OM that lacks a distinct shape, outline and structure (Tyson, 1995; Atta-Peters et al., 2013). The non-pollen palynomorphs (NPP) in the palynofacies include fungal and algal remains (Appendix 1).

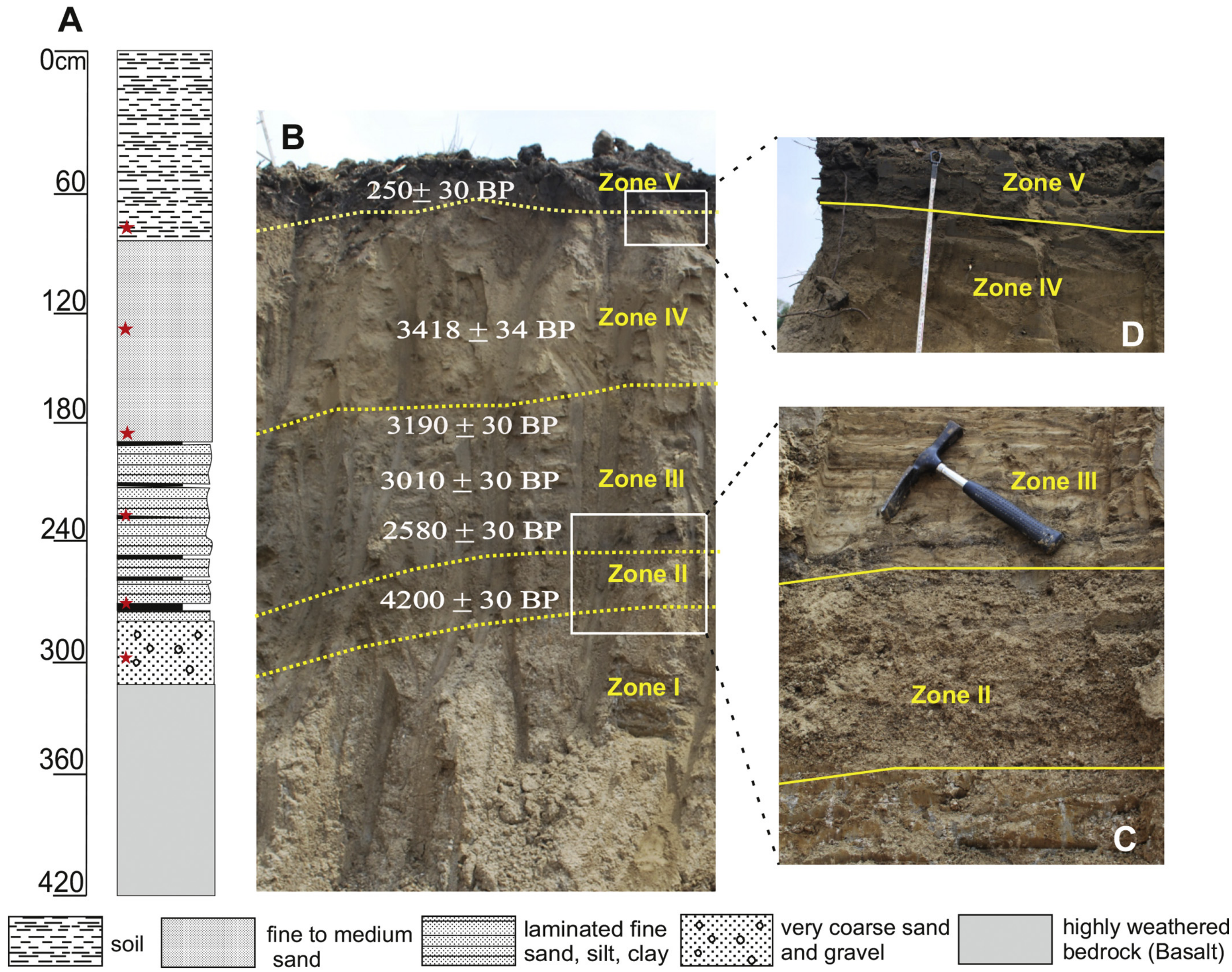

Fig. 2. A. Litholog of the sediment sequence revealing five distinct zones. B. A close view of the section with chronology. C. Photograph showing the sharp contact between coarse sand zone II and the fine sand zone III. D. Photograph showing the sharp contact between the zone IV and soil horizon V.

48 samples (BK 1d - BK 44) barring the four samples from the weathered basalt zone were analysed for palynofacies. The samples were treated with HCl (10%) and HF (40%) to dissolve carbonates and silicates. To analyse the entire OM and ensure no alteration of OM preserved during chemical processing, use of oxidizing reagents (KOH and HNO_3) was avoided. The samples were sieved using 500 mesh (~25 µm) and dispersed on glass slides using two drops 3% polyvinyl alcohol (PVA) and finally mounted with Canada Balsam. After the slides were prepared and dried, these were scanned under the transmitted light microscope Olympus BH2 (20× and 40×) and 300–500 palynofacies components were counted and the photography was done on DP25 camera. The palynofacies data obtained on sediment samples was transformed into relative percentage based on the abundance and predominance of the particulate OM. Further, the data were subjected to Tilia 1.7 software for constrained CONISS cluster analysis (Fig. 4) given by Grimm (1987, 1990). The important palynofacies are represented in Fig. 5. The analyses were performed at the Birbal Sahani Institute of Palaeosciences, Lucknow, India.

3.3. Mineral magnetic measurement

Mineral magnetic properties of sediments have been used as proxy to decipher palaeoenvironments and climate change. Magnetic measurements have also been applied to flood records wherein the minerogenic flood layers are seen to possess high content of magnetic minerals. Magnetic minerals in the natural environment are highly sensitive to changes in environmental conditions. They are therefore extremely useful palaeoenvironmental and palaeoclimatic indicators (Thompson and Oldfield, 1986; Basavaiah, 2011). In the present work, the bulk magnetic properties such as Magnetic Susceptibility (χ), Anhysteretic Remanent Magnetization (ARM) and Isothermal Remanent Magnetization (IRM) of lacustrine sequences were studied with an aim to apply such information to flood records wherein the minerogenic flood layers are seen to possess high content of magnetic minerals.

A total of 48 samples (BK 1 - BK 48) were subjected for room temperature magnetic measurements at the Environmental Magnetism Laboratory, Indian Institute of Geomagnetism, Navi Mumbai. The samples were normalized for differences in density by dividing by each sample's dry weight. The description of the parameters measured, and their possible inferences are given in Appendix 2. Mass-specific χ was measured using a MFK1-FA Kappabridge at low frequency (976 Hz) and high frequency (15,616 Hz). Frequency-dependent susceptibility (χfd %) was determined by the difference between the high and the low frequency measurements as a percentage of χ at low frequency, ARM and IRM were measured on a Molspin magnetometer. Peak induction for ARM was l00mT, with a D.C. bias of 0.05mT using ASC Scientific D-

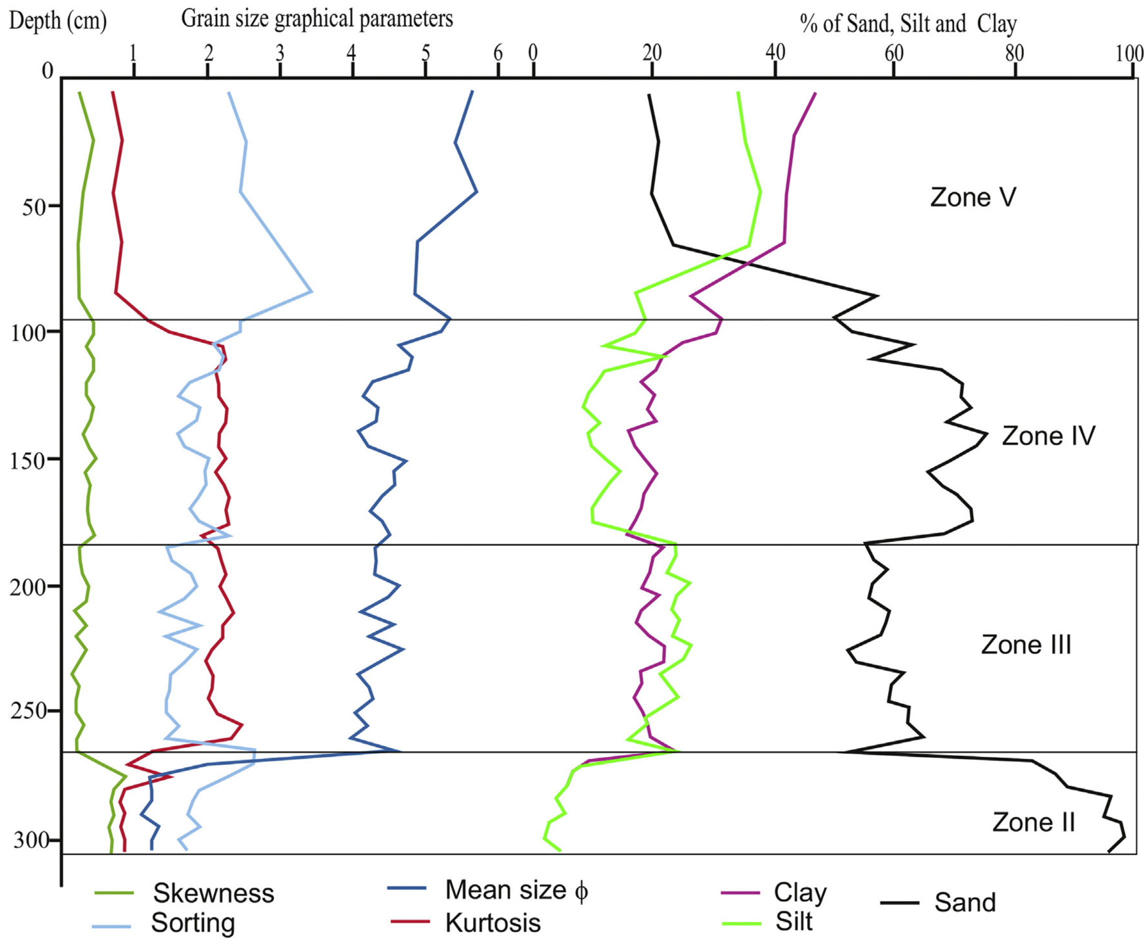

Fig. 3. Plot showing sediment mean size, sorting, skewness, kurtosis values and sand percentage variations with depth.

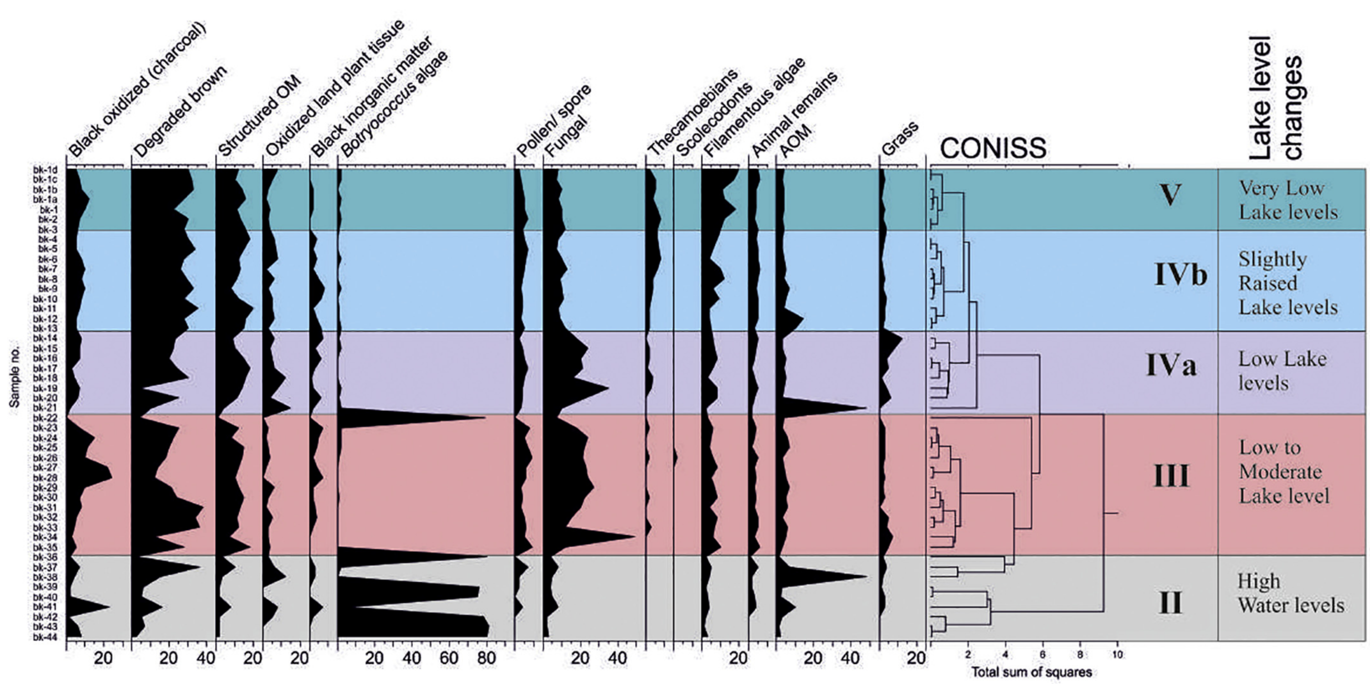

Fig. 4. Plot of palynofacies distributions in various litho units and zonation based on CONISS cluster analysis.

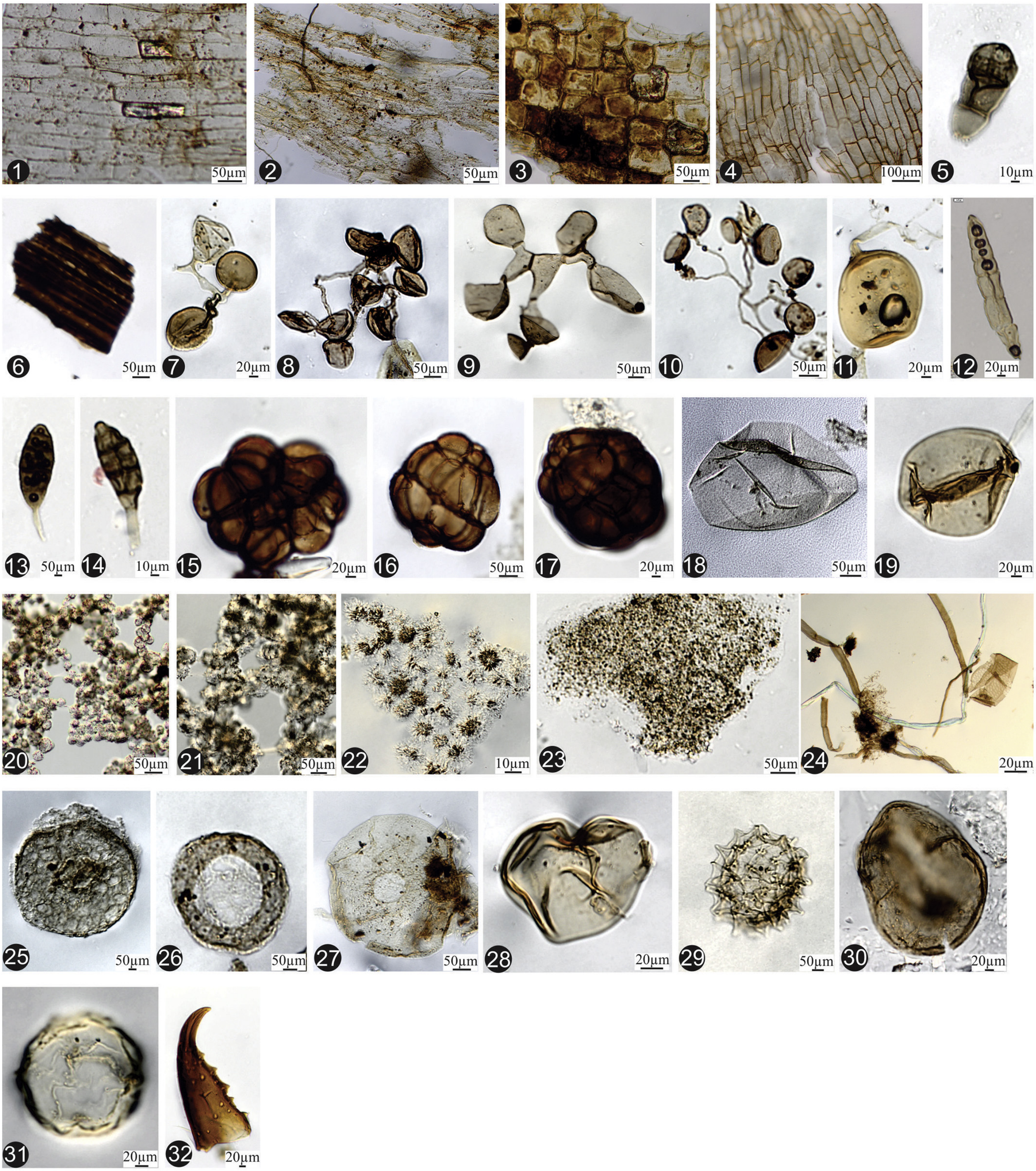

Explanation of Plate I

1-4: Structured organic matter; 5, 12-14: *Alternaria* sp.; 6: Degraded brown organic matter; 7-11: *Glomus* sp.; 15-17: *Acacia* sp. ; 20-22: *Botryococcus* alga; 23: Amorphous organic matter (AOM); 24: Filamentous algae; 25-27: Thecamoebians, 28-31: Spore; 32: Scolecodont

Fig. 5. Plate with photomicrographs of the significant palynomorphs.

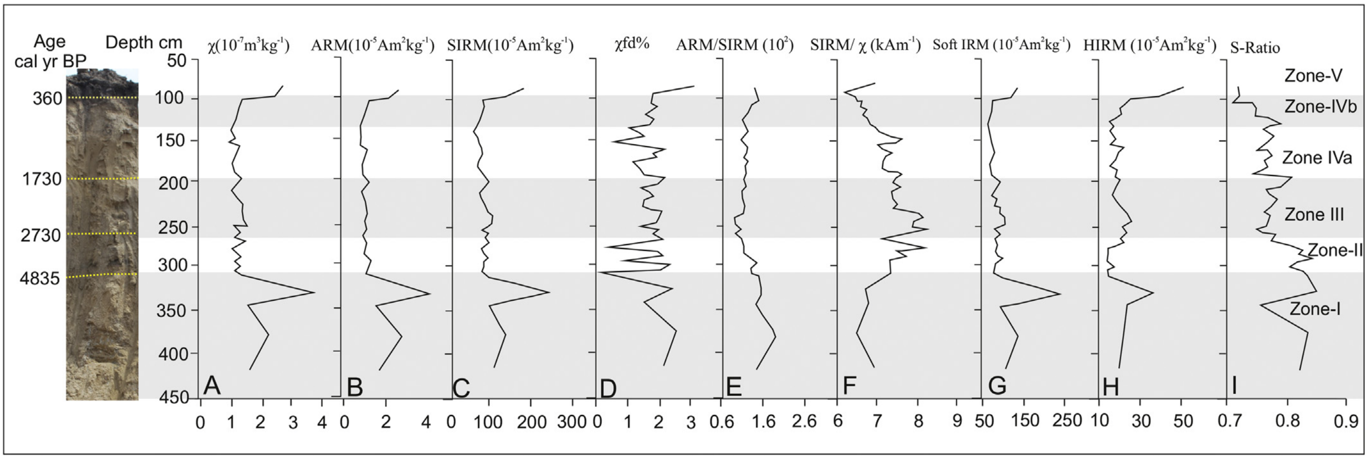

Fig. 6. A–I. Plots showing variations in the mineral magnetic parameters (χ, ARM, SIRM, χfd%, ARM/SIRM, SIRM/χ, Soft IRM, HIRM and S-ratio). The colour zones across the plots demarcate the depositional zones I–V.

2000 AF demagnetizer. Initial IRM was imparted with Molspin impulse magnetometer in the 1 T forward field and is termed as Saturation IRM (SIRM). Opposite (back) IRM was imparted in 0.03, 0.06, 0.1 and 0.3 T field (Thompson and Oldfield, 1986; Basavaiah, 2011). Magnetic susceptibility is mainly a measure of magnetite concentration, when magnetite is present. Therefore, the IRM and ARM results were divided by χ in order to obtain a measure of magnetic characteristics that are independent of magnetite concentrations, such as magnetic grain size and mineralogy. The magnetic grain size effect is seen in the ARM/χ and SIRM/χ as higher values with greater amounts of fine magnetic material. SIRM and back-IRM distinguishes high-coercivity magnetic minerals, such as hematite from low-coercivity magnetic minerals, such as magnetite and Ti-magnetite. Derived magnetic parameters from the measurements include HIRM (=SIRM-$IRM_{-0.3T}$) and Soft IRM (=SIRM-$IRM_{-0.02T}$), which indicate the amount of hematite, Ti-magnetite and magnetite in the sample respectively. The S-Ratio (King and Channell, 1991; Basavaiah and Khadkikar, 2004) was calculated from the SIRM and back-IRM results: S-Ratio = $IRM_{-0.3T}$/SIRM (1 if no hematite; < 1 if hematite present). The results of the analysis are plotted in Fig. 6 corresponding to five lithostratigraphic and pollen zones (I–V). Visual interpretation and mineral magnetic investigations suggested these subdivisions based on the composition of magnetic minerals (Soft IRM, HIRM and S-Ratio) and magnetic grain size characteristics (ARM/SIRM and SIRM/χ) (Fig. 6). The significance of these parameters in inferring the palaeoenvironments is summarised in Appendix 2.

3.4. Analysis of elemental concentration

Elements like Si, Al, Fe, K, and Ti have high concentration in the detrital sediments and therefore used to identify detrital layers in the lacustrine archive (Revel-Rolland et al., 2005). Elemental analysis was done for 24 representative samples for which about 1 g of the powdery material (< 63 μm fraction) of the crushed samples in a mortar was placed into a small circular cup, sealed by a polypropylene membrane. Each time, 12 samples were placed in a sample tray and subjected to X-ray fluorescence (XRF) analysis using the SPECTRO XPOS at the environmental magnetism laboratory, Indian Institute of Geomagnetism, Navi Mumbai. The range of elements that can be measured is from sodium (Na) to uranium (U). The spectra of samples were evaluated using the supplied 'Turboquant' program, and eleven elements namely Si, Ti, Zn, Al, Fe, Zr, Sr, Ca, K, Na and Ba were determined for this study (Fig. 7). The accuracy of measurements was checked by GBW-07401 Geochemical Standard Reference Soil Sample and the precision was better than 2%.

3.5. Radiocarbon chronology

Six bulk organic carbon sediment samples were identified for accelerator mass spectrometry (AMS) ^{14}C dating of which five were analysed at the Beta Analytic Testing Laboratory in USA and one at the Physical Research Laboratory, Ahmedabad, India. Bulk sediments were chosen for AMS dating as macrofossils are found not only in very few horizons but also in a meagre quantity. Since the sediments are also derived predominantly from the lake catchment with terrestrial plant remains, it may lead to younger ages (Oswald et al., 2005).The organic fraction from the bulk sample that remains after sieving the sediment to < 180 μm to remove any roots or macrofossils and then acid washed to remove carbonates of the sample was dated. The AMS Radiocarbon ^{14}C ages were calibrated in OxCal v.4.2 package (Bronk Ramsey, 2001) with the standard IntCal 13 calibration curve (Reimer et al., 2013) and referred as calibrated years B.P. (cal yr B.P.) in a range of ± 10 years (Table 1). An age-depth model was produced using the Poisson process depositional model which is highly tangible for non-uniform depositional rate and proves to be more realistic in simulating the depositional history (Bronk Ramsey, 2008).

Six AMS radiocarbon dates obtained on the sediment succession of the Timbi Lake are 4240 ± 30 yr BP, 2580 ± 30 yr BP, 3010 ± 30 yr BP, 3190 ± 30 yr BP, 3418 ± 34 yr BP and 250 ± 30 yr BP at 280–295, 260–265, 210–235, 190–195, 120–135 and 80–90 cm depth respectively (Fig. 2, Table 1). Older dates within the sediment sequence at the depth of 210–235, 190–195, 120–135 cm are observed. These horizons represent the reworked sediments from the catchment with older carbon depleted in 14C and have been excluded from the age-depth model. The age inversion in the Timbi Lake is attributed to episodic sediment focusing events that reworked the older material from the catchment during high discharge floods and deposited in the lake. The systematic inversion of the ages observed in zone III and IV within organic and inorganic sediment layers suggests a mechanism of sediment deposition wherein both erosion and deposition occur simultaneously (Brown et al., 2002). Bierman et al. (1997) suggest that scouring and erosion of sediments from the lake margins and subsequent redeposition would lead to the inversion of ages. Extrapolation of ages was done based on age–depth model (Fig. 8; Table 1) with lighter and darker shades indicating 95% and 68% probability ranges respectively (Reimer et al., 2013; Bronk Ramsey, 2017).

4. Results and interpretations

Based on the interpretation of the multiple proxies, the sediment succession at the Timbi Lake was divided into five zones of sediment

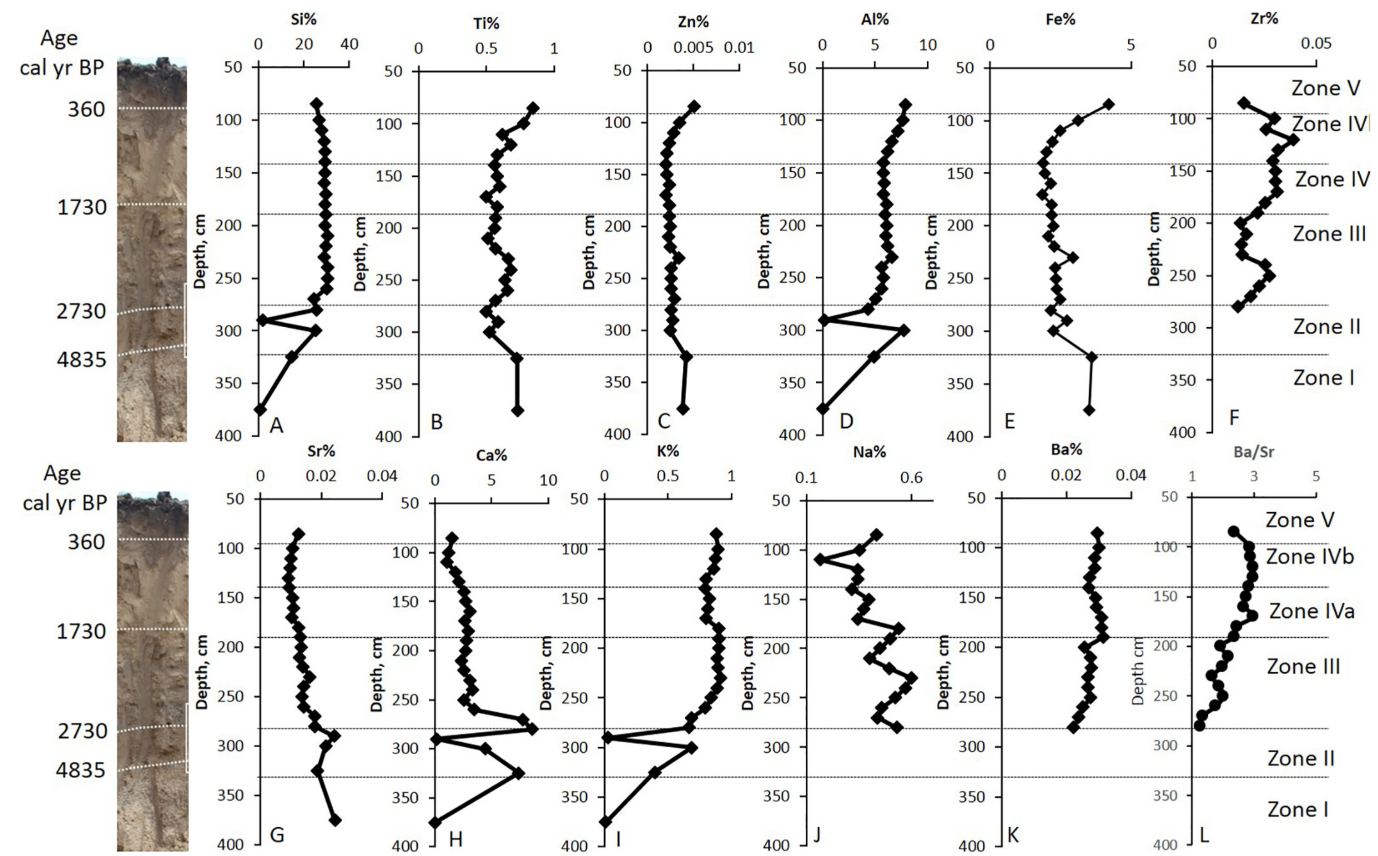

Fig. 7. A–L. Plots representing the variation in elemental concentrations in the sediments during various depositional zones.

Table 1
Conventional and calibrated ^{14}C dates of the Timbi lake sequence.

Depth range (cm)	AMS age (yr)	Error (yr)	Calibrated age cal B.P.	Median cal B.P.	Based on sed. rate
80–90	250	30	324–271	298	298
120–135	3418	34	3614–3701	3667	881
190–195	3190	30	3463–3361	3412	1771
210–235	3010	30	3271–3140	3178	2183
260–265	2580	30	2763–2699	2731	2731
280–295	4240	30	4860–4810	4835	4835

deposition (Figs. 2–4, 6–7) as described below.

4.1. Zone I (BK 45 - BK 48; 305–420 cm depth)

This zone comprises weathered basalt, greyish brown in colour showing mottling and vertic character over which the sediment sequence lies (Fig. 2A). The weathered basalt samples were found unsuitable for grain size and palynofacies analysis. The mineral magnetic analysis shows high values of all magnetic proxy parameters such as χ, ARM, SIRM, χfd%, ARM/SIRM, Soft IRM, HIRM and S-Ratio (Fig. 6A–I). The elemental concentrations of Ti, Zn, Al and Fe are high (Fig. 7B–E) and there is complete absence of Zr, Ba, and Na (Fig. 7F, J, K). The high values of magnetic parameters indicate pedogenesis by subaerial exposure (Jain et al., 2005), which promote mechanical weathering and erosion. The weathered nature of basalt is also suggested by the concentration of immobile elements such as Fe, Al and Ti and depletion of mobile elements such as Na, Ba and Zr (Das and Krishnaswami, 2007).

4.2. Zone II (BK 36 - BK 44; 265–305 cm depth)

The zone II corresponds to a 40 cm thick layer of coarse sand and fine gravel with occasional cross stratifications overlying the weathered basalt with a sharp contact (Fig. 2). The sediment grain size varies between coarse sand to fine gravel with mean size of 1.2Ø, is poorly sorted (Fig. 3), mesokurtic and very fine skewed. In lake catchments, any change in the hydrological activity is reflected in the size of the clastic component of the sediments and has been widely used as a proxy (Bøe et al., 2006; Kuzucuoglu et al., 2011; Schillereff et al., 2014). The rainfall and runoff intensity control the sediment grain size, wherein higher rainfall and runoff is linked with coarser terrestrial particles. The deposition of coarse particles shows a positive relationship with the high discharge conditions (Campbell, 1998). The very fine skewed character and the particle size of the sandy gravel suggests a predominant gravel mode with a subordinate sand mode of riverine input (Folk and Ward, 1957). Poor sorting suggests that sediments have not undergone extensive post-depositional reworking (Bøe et al., 2006).

The palynofacies study indicates that in this zone, *Botryococcus* algae is represented in very high percentage (75 to 80%) except in three samples (BK-37, 38 and 41 i.e. < 5%; Fig. 4). The phytoclasts remains comprising of degraded brown varies from 2% to 36% while the black oxidized charcoal ranges between 2 and 23%. The structured OM and oxidized land plant remains vary from 2% to 12% and are absent in samples (BK 44, BK 43, BK 40 and BK 39). The pollen/spore and fungi percentage are very low (2–7%). The filamentous algae, chitinous animal-remains and oxidized grass cuticle are represented below 5% and AOM is < 10%.

The *Botryococcus* alga bloom in inland, shallow and oxygenated freshwater lakes, ponds, pools suggesting its formation in stagnant water and low energy conditions (Guy-Ohlson, 1992; Demetrescu, 1998). The low turnout of the phytoclasts is attributed to nutrients from

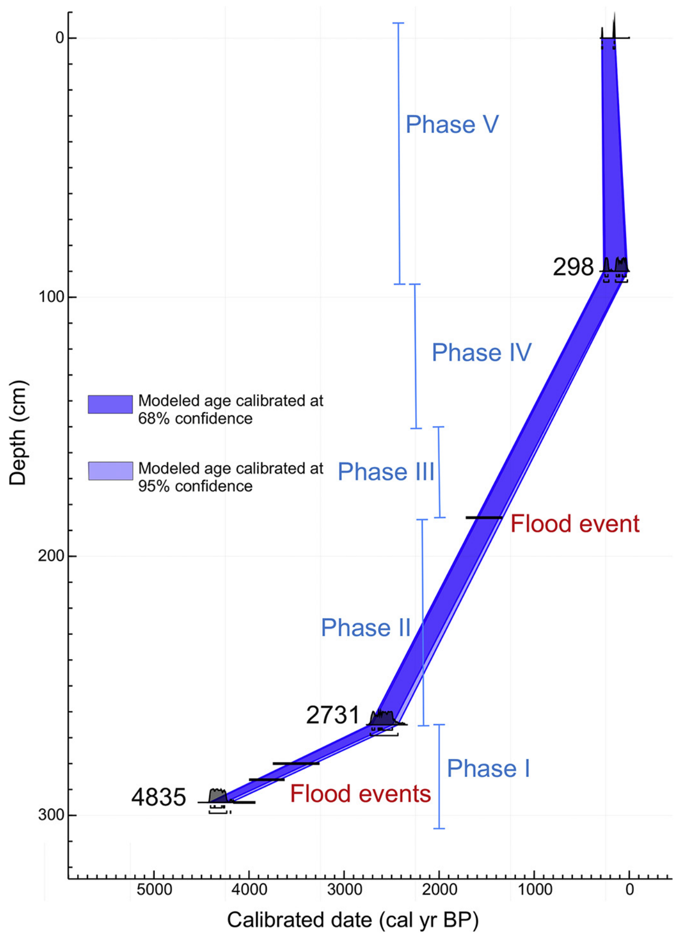

Fig. 8. Fig. 4. Age-depth graph for the Timbi lake based on AMS ^{14}C chronology and calibrated based on OxCal v4. 3. 2 (Bronk Ramsey, 2017); r: 5 IntCal13 atmospheric curve (Reimer et al., 2013). Also marked are the phases of deposition and the flood events.

terrestrial supply that allowed blooms of *Botryococcus* alga during the deposition time and developed an oligotrophic condition in the riverine complex (van Geel, 1978; Tunno and Scott, 2017). However, the presence of *Botryococcus* alga in alternate layers (Fig. 2) suggests occurrence of multiple high energy discharge events followed by periods of relatively low hydrological activity in the catchment. It is also seen that in sample BK-41, BK-38 and BK-37 when the *Botryococcus* alga is in very low or negligible percent, the brown degraded matter, charcoal and AOM show high concentration (Fig. 4). The variation of the charcoal components indicates transportation of plant material from the catchment during events of high runoff wherein the terrestrial influx at large allows the transport and degradation of particulate OM.

The χ, ARM and SIRM values in zone II are lower compared to zone I, indicating less concentration of ferrimagnetic minerals. The sharp and gradual decrease in χfd% and ARM/SIRM respectively at the contact of zones I and II is observed and signify a shift from fine-grained magnetic minerals to relatively coarser magnetic grain size (Fig. 6). χfd% shows fluctuating behaviour, while ARM/SIRM shows a gradual decrease in value upwards. The χfd% values with low spikes for sample BK 41, BK 38 and BK 37 (Fig. 6) suggest high runoff in tune with the inference from the palynofacies. The higher values of ARM/SIRM suggest abundant erosional debris dominated by finer magnetic grains. Moreover, the χfd% and SIRM/χ values show variability and show peaks in Soft IRM and HIRM data, indicating contribution of sediments from the catchment with change in hydrology (Basavaiah and Khadkikar, 2004). The increase in S-Ratio and distinct decrease in magnetic concentration at beginning of this phase indicate a change in the sediment character (Fig. 6H–I) from the underlying basalt basement (Fig. 2). The high-coercivity magnetic minerals (e.g. Ti-magnetite and hematite) were derived from the weathering of Deccan basalt in zone I (Thompson and Oldfield, 1986; Basavaiah and Khadkikar, 2004; Oldfield, 2007; Basavaiah et al., 2010, 2015) and hence their contribution to the sediment load decreased in zone II. The presence of coarse grained multidomain (MD) or pseudo-single domain (PSD) magnetic minerals as exhibited by decrease in ARM/SIRM and χfd% (Fig. 6D, E), corroborate the interpretation that the sediments represent detritus eroded from the catchment.

Further, the sediments contain higher Si and K contents (Fig. 7A, I), lower Ti and Fe concentrations compared to underlying weathered basalt zone suggesting terrestrial input from the catchment. The onset of lacustrine environment is reflected by the occurrence of elements Zr, Ba, Br and Na at the end of this phase. The higher concentration of Ca, Na and low Ba/Sr ratios (Fig. 7H, J, L) suggest low intensity leaching and shallow water conditions during arid climatic conditions (Gallet et al., 1996).

Zone II thus represents a phase of high energy river flooding with three peaks as is evident from the coarse sediment character, high ARM/SIRM and χfd% magnetic parameters and high degraded brown matter, charcoal and AOM. The flooding was followed by phases of water stagnation allowing Botryococcus blooms (Guy-Ohlson, 1992; Demetrescu, 1998). Flood sedimentation resulted in channel infilling marking the end of this phase as seen in the changed sediment character and a sharp contact between the sediments from the succeeding zone III (Figs. 2A, B and 3).

4.3. Zone III (BK 22 - 35; 185–265 cm depth)

The zone III comprises 80 cm thick horizon of very fine sand and silt. The sediments show horizontal laminations and intercalation of minerogenic and organic rich silt layers (Fig. 2C). Six layers of silty sand 10–20 cm thick can be demarcated, each followed by a thin (about 2 cm) organic rich layer. The mean size of sediments varies between 4.1 and 4.5 ø, sorting is poor, sediments are fine skewed and very leptokurtic in character (Fig. 3). The sediments show a bimodal distribution with predominant saltation and suspension populations (Supplementary Figs. 1 and 2). High kurtosis and skewness values are interpreted as indicating that a large amount of reworking has taken place in and adjacent to the point of deposition of the sample (Cadigan, 1961).

This zone exhibits high percentage of phytoclasts dominated by degraded brown, structured organic matter and black charcoal varying from 2% to 38%. The phytoclasts remains can be identified as belonging to herbs and shrubs derived from the close catchment near the water body. There is a decline in the woody remains in the phytoclasts components. Further it may also be noted that the fungal remains show high percentage varying from 7% to 50% and consist of high percent of *Glomus* sp. (Figs. 4 and 5) in this zone. The filamentous algae also show variability from 3% to 10% in this zone. The *Botryococcus* alga are low; but in BK-22 it represents about 79%. The AOM in this zone is below 7% while the oxidized grass remains varies differently from 2% to 7%.

The various palynofacies components viz. degraded brown, structured OM and high fungal remains suggests prevalence of aquatic conditions. The palynofacies and non-pollen palynomorphs (*Glomus* sp., *Alternaria* sp.) assemblage suggests a stagnant water body or a lake deposit (van Geel et al., 2011; Quamar, 2015) with limited runoff from larger distances. The dominance of *Glomus* sp. (Fig. 4) indicates possible erosion from the local catchment area and sediment infill from lake edges (Quamar, 2015). The reduction in the woody phytoclasts suggests periods of low precipitation and shallowing of the lake. The high percentage of *Botryococcus* alga in BK 22 (Figs. 2A and 4) indicates an influx of freshwater possibly due to flash flooding and later stagnation that marked the end of the phase.

The sediments correspond to low χ, ARM, SIRM, Soft IRM and S-Ratio (Fig. 6A, C, E, I), suggesting a high concentration of high-coercivity magnetic minerals and/or paramagnetic minerals (Sandgren and Snowball, 2001). The high content of antiferromagnetic (e.g. hematite) and high-coercivity ferrimagnetic (e.g. Ti-magnetite) minerals within the zone III appear consistent with higher HIRM and SIRM/χ ratios and share elevated Ti, Zr and Ba concentrations (Fig. 7B, F, K). However, the increase in S-Ratio at the termination of the phase, not supported by Soft IRM, is associated with low χfd% and SIRM/χ ratio values, probably results from early lake sediment deposition of coarse grained (MD) ferrimagnetic minerals such as magnetite and Ti-magnetite derived from eroded soils and share high Ti and Zr contents (Fig. 7B, F) corresponding to the flooding event at the transition from zone III to IV. Overall low ARM/SIRM and χfd% suggest MD component consistent with inputs from the catchment derived deposition of detrital magnetic minerals (Basavaiah et al., 2004; Bøe et al., 2006). The higher precipitation, warm climatic conditions and high bank erosion during this phase led to a change in the concentration of magnetic minerals due to a shift in allochthonous sediment in-wash from the catchment (Basavaiah et al., 2004, 2010). The Zr/Fe ratios have been used as particle size proxies (Wilhelm et al., 2013) and indirect indicators for deposition processes. The higher Zr/Fe ratio here suggests predominance of silt-sand fraction over the finer particles and thus terrestrial influx. Improved moisture content, humid climatic conditions and stable lake levels can be inferred from the observed increase in concentration of K and Ba/Sr ratio (Fig. 7I, L) and a corresponding decrease in Na and Ca content.

The zone III thus represents the development of a palaeo-lake during enhanced precipitation with a shallow but stable lake level wherein deposition of finer authigenic sedimentation took place. There were however periods of high terrestrial influx and enhanced lake margin erosion corresponding to flooding events.

4.4. Zone IV a and b (BK 3 - BK 21; 90–145 and 145–185 cm depth)

The overlying unit is 95 cm thick and comprises massive silt and very fine sand (Fig. 2B). The sediment mean size is between 4.2 and 4.8 ø, poorly sorted, very fine skewed and very leptokurtic (Fig. 3). The size distribution shows bimodality (Supplementary Figs. 1 and 2), saltation being the dominant means of transport. There is an increase in the sand content and a corresponding decrease in the clay and silt content as compared to the underlying zone III (Fig. 3). The very leptokurtic character is due to the presence of predominant fine sand mode with a subsidiary clay and silt mode (Friedman, 1961). The very fine skewness suggests a riverine input and low energy conditions. Higher skewness values of finer sediments have been attributed to low lake levels and intensive transport with riverine admixture in the lake sediments (Liu et al., 2016).

Relatively low values are observed in all magnetic concentration parameters throughout the zone IV (Fig. 6). The lower and constant values of χ, ARM, SIRM, Soft IRM and ARM/SIRM parameters do not agree with the gradual decrease of SIRM/χ values indicating increase in contribution of paramagnetic component (Oldfield et al., 1983; Lepland and Stevens, 1996). Lower S-Ratio do not show higher HIRM values that may be consistent with a mixture of higher proportions of high-coercivity magnetic minerals (e.g. Ti-magnetite and minor hematite) suggesting a low fluvial input during this phase. The geochemical indicators of Fe, Al, Ti, Zn, Zr and Br show similar trends to zone III in their elemental concentrations (Fig. 7B–F) associated with the high-coercivity ferrimagnetic Ti-magnetite and antiferromagnetite hematite and paramagnetic minerals. The fluctuating Ba/Sr ratio with a gradual increase towards the top and decrease in the Ca values (Fig. 7H, L) suggest higher precipitation and deeper lake levels (Gallet et al., 1996). Overall the sediment composition shows greater amounts of high coercivity magnetic minerals and paramagnetic minerals deposited into the lake under high monsoon variability and fluctuating lake levels.

Based on the palynofacies components, the zone IV is further divided into two, zone IVa and IVb. In the zone IVa the phytoclast components comprising of degraded brown range from 10% to 30% and the overall charcoal component is lower than 10% (Fig. 4). The structured OM (Fig. 5) also vary from 10% to 20% with a low at 190 cm (4%). The oxidized land plants vary as low as 8% in most of the samples with a slight peak at 190 and 175 cm where they range from 12 to 15%. The black opaque particles, *Botryococcus* alga and pollen/spore percentage is low (< 5%). The fungal remains comprise of *Glomus* sp., *Tetraploa* sp., *Alternaria* sp. (van Geel et al., 2011; Quamar, 2015; Tunno and Scott, 2017). The Thecamoebians, filamentous algae and animal remains (Fig. 4) are present (up to 10%) and AOM ranges < 5% in most of the samples except at 190 cm (48%) and 150 cm (10%). The oxidized grass remains is also present in low percent ranging from 1% to 12%.

The high AOM content in the bottom sediments points towards higher degradation of OM due to oxic environmental conditions (Traverse, 1994; Tyson, 1995; Hoaen, 2000; Tyson and Follows, 2000). The higher percentage of brown degraded palynofacies component and fungal remains in the sediments point towards water table fluctuations in the lake. The effect of bank erosion under warm and dry climate can be indicated due to presence of *Glomus* sp., *Tetraploa* sp. and *Alternaria* sp. (Quamar, 2015). The reduced percent of black oxidized charcoal particles may be inferred as the reduction in biomass with a shift from trees to shrubs and herbaceous plants (Fig. 4) indicating a transition towards dry climatic conditions. The degraded brown also shows presence of shrubs and herbaceous plant remains rather than woody particles. The structured OM in the zone also suggests preservation of herbaceous plants under well-oxygenated conditions.

The zone IVb comprises of high percent of degraded brown phytoclasts (25% to 35%) along with low to moderate percentage of structured OM (8% to 18%) with low turnout of black oxidized charcoal components (Fig. 4). The oxidized land plant tissue, opaque (inorganic) phytoclasts remains, pollen/spore and *Botryococcus* alga are also low ranging from 1% to 8%. Further the fungal remains also vary from 7% to 13% with presence of *Glomus* sp., *Tetraploa* sp., *Alternaria* sp. (Fig. 5) while the Thecamoebians range between 2% to 8% which is higher than all other zones. The filamentous algae vary between 4 and 12% whereas the animal remains, and oxidized grass remains are < 5%. The AOM shows very low percentage in this zone (< 5%) except at 145 cm where it ranges about 12%.

The higher percentage of degraded brown and structured OM indicate higher lake waters which may be due to moderate to higher periods of southwest (SW) monsoon (Prasad et al., 2014a). It is also pertinent to note that the degraded OM consists of herb and shrub type of plant remains which indicates that the monsoon may have enhanced during the depositional phase but not to the extent that it may have helped in flourishing the woody forested biomass. The lowering of the fungal remains in this zone (Fig. 4) points towards moderate to higher water level in the lake and weak to moderate energy conditions. The variation in the Thecamoebians and filamentous algae and their moderate increase points towards pristine water with good oxygenation conditions. The lowered values of oxidized grass remain indicate lack of preservation due to higher water levels in the lake.

Thus, based on the proxy records it is inferred that deposition in this zone represents stable monsoon conditions with low energy flows but steady fluvial input to the lake resulting in the deposition of finer sediments and palynomorphs which survive in fresh water and well-oxygenated conditions.

4.5. Zone V (BK 1d - BK 2; 0–90 cm depth)

The topmost zone (zone V; 0–90 cm) comprises pedogenised organic rich sediment, dark in colour (Fig. 2D). The Mz is ~4.8 and sediments show very poor sorting (Fig. 3), fine skewness and platykurtic nature. The size distribution shows unimodality with a major bedload population.

The degraded brown phytoclasts show high presence of herbaceous remains and very low shrubs and woody fragments. Similar are the observations for the black oxidized charcoal components which primarily consist of herbs and extremely low woody fragments. The moderate to high percent of filamentous algae (Fig. 4) indicates very low water levels and formation of soil or clay rich in organic matter and water nutrients. Further the abundance of filamentous algae points towards enhanced human activity and eutrophication in the lake. The well-preserved structured OM indicated good preservation potential of herbs and shrub plants.

A slight increase in magnetic concentration is noticeable in the topmost zone V, both χfd% and SIRM/χ show a slight increase while ARM/SIRM show no such variation (Fig. 6D–F). Soft IRM and HIRM values are high and S-Ratio values reduce to below average (Fig. 6I). This indicates that the sediments contain a mixture of the naturally weathered and unweathered magnetic minerals characterized by ferrimagnetic and antiferromagnetic components reflecting the potentially mixed origins of magnetic minerals in sediments which may have an anthropogenic, natural or mixed source. This zone is characterized by higher concentrations of Fe, Ti and Zn compared to the other zones (Fig. 7). Lower Ba/Sr ratio indicates low humidity conditions.

5. Discussion

5.1. Phases of sediment deposition and flooding events

Based on the proxy data and chronology, five major depositional phases corresponding to the zones (II, III, IV a, IV b and V) of the Timbi lake described in the Results section and major flood events therein have been demarcated (Fig. 9). The Phase-1 has been interpreted as a phase of high energy fluvial sedimentation. The peaks in grain size, S-Ratio and lows in χfd% (Fig. 9) represent three distinct flood pulses around 4800 cal yr B.P. that correlate with flood events reported from the slackwater deposit records of the Mahi River at around 4.6 ± 1 ka (Sridhar, 2007a, Fig. 10). Higher percentage of degraded brown matter, charcoal and AOM also suggest high runoff and terrestrial influx (Fig. 4). The abundance of *Botryococcus alga* in the intervening layers indicate shallow, stagnant water conditions and relatively low hydrological activity in the catchment (Tunno and Scott, 2017) following each flood event (Fig. 9). The poor representation of pollen/spores as well as land plant tissue in the sand layers suggests deposition under dry climatic conditions. Higher concentration of Ca and low Ba/Sr ratios during phase I also suggest shallow water and dry climatic conditions (Gallet et al., 1996). We thus infer that during phase I, though the climatic conditions were largely dry and the monsoon weak, flash flooding in the catchment led to the deposition of sediments. If we try to understand the occurrence of flood events in the context of the monsoon strength, it is evident that the flood events reported ~4800–4600 cal yr B.P. have occurred during the period of arid conditions or more possibly, towards the transition from arid to humid phase (Sridhar and Chamyal, 2018). Giosan et al. (2012) have also indicated large scale flooding prior to mature Harappan stage (4600–4200 B.P.) and a subsequent decrease in the flooding intensity based on the landscape studies of Hakra-Ghaggar and Indus rivers located to the north of the Timbi Lake.

The phase I of the Timbi lake around 4800 cal yr B.P. can be correlated with the phase of weakened monsoon and dry climatic conditions in the Pariyaj lake between ~5864 and 4680 cal yr B.P. (Fig. 10, Raj et al., 2015), Lunkaransar and Didwana at ~5000 and ~4700 cal yr B.P., Sambar lake at ~4700 cal yr B.P. (Prasad and Enzel, 2006) and Wadhwana lake between 5560 and 4255 cal yr B.P. (Fig. 10; Prasad et al., 2014a). Correlated marine records from the Arabian Sea point towards the onset of dry climatic conditions in India around 5000 cal yr B.P. (Staubwasser et al., 2003; Gupta et al., 2003). The records from neighboring Wadhwana lake show a gradual strengthening of SW monsoon only after ~3500 cal yr BP with once again a short pulse of dry climatic conditions (~3238 to ~2709 cal yr B.P. Prasad et al., 2014a).

The Timbi Lake records show a period of erosion between phase I and the beginning of phase II (2730 cal yr B.P.) as observed in the sharp contact and a distinct change in the sediment character from riverine to lacustrine (Fig. 2A & B). The abandonment of the channel and transition to lacustrine environment may be attributed to climatic or tectonic changes in a region (Schillereff et al., 2014). However, the absence of tectonic indicators and the prevalence of aridity across the region as suggested by the palynofacies and magnetic parameters in the Timbi lake indicates that the channel probably became defunct due to lack of flow under reduced precipitation and isolated water bodies were formed (Fig. 2D) in the area. Reorganisation of channels and change in the sediment facies from fluvial to lacustrine has been recorded in various nearby ponds in the drainage basin (Raj, 2004). The rejuvenation of monsoon occurred around 2730 cal yr B.P. as also recorded in the Pariyaj and Wadhwana lakes (Raj et al., 2015; Prasad et al., 2014a). Earlier studies on the marine records from the Arabian Sea have also indicated high southwest monsoon precipitation at 2.8 ka (Anderson et al., 2010; Gupta et al., 2003; Tiwari et al., 2006).

The decrease in the sediment grain size, increase in the fungal remains and reduction in woody phytoclasts mark the beginning of phase

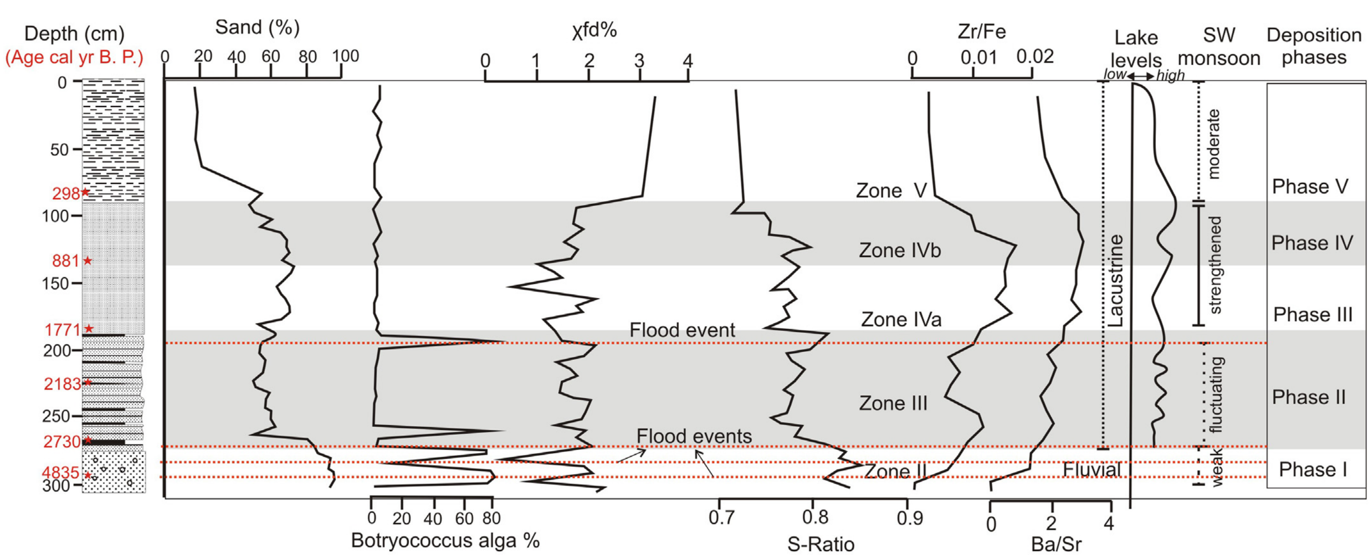

Fig. 9. Compilation of major proxy parameters used for inferences on palaeofloods and palaeo environments - sand percent, Botryococcus alga, χfd%, S-Ratio, Zr/Fe, Ba/Sr, inferred lake levels, south west monsoon intensity and depositional phases from the Timbi sediment sequence.

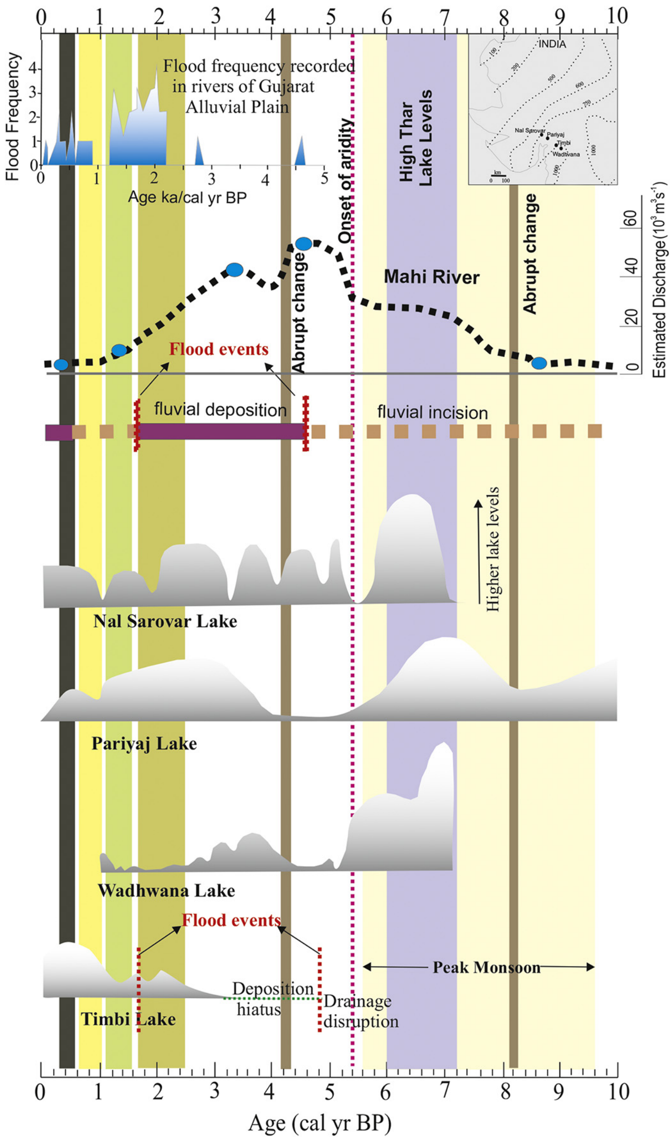

Fig. 10. Summary figure showing the correlation between the flood events in the Gujarat Alluvial Plains, Indian Summer Monsoon activity and the Lake levels in western India. The levels for the Wadhwana, Pariyaj and Nal Sarovar lakes are based on Prasad et al. (2014a), Raj et al. (2015), Prasad et al. (1997) and redrawn from Raj et al. (2015). The phases of peak monsoon, high Thar lake levels and abrupt climatic changes have been marked from Kale et al. (2003). The flooding pattern and discharge of the Mahi River is represented based on Sridhar (2007a, 2007b). The flood frequency recorded from fluvial archives of alluvial plains is shown from Sridhar and Chamyal (2018). Note that the flood events identified from the Timbi lake sediments in the present study corroborate well with the fluvial archives in the region.

II around 2730 cal yr BP (Fig. 4) indicating low but stable water levels with limited runoff and low precipitation. Data on chronology shows that the sediment layers have yielded successively older ages dating to 3180 ± 30 and 3410 ± 30 cal yr B.P. suggesting reworking of sediment and incorporation of older carbon. According to Brown et al. (2002) the inversion of ages also indicates that both erosion and deposition mechanism are involved in the emplacement of these layers. These sediment layers probably point towards higher erosion and sediment movement from a larger catchment leading to periodic infill to the lake during enhanced monsoon (Schillereff et al., 2014). During this phase, periodic sediment influx from catchment occurred, perhaps during pulses of higher precipitation at 2730, 2490, 2285, 2150, 2010 and 1875 cal yr B.P. (Figs. 2A & 3) as evident in the dominance of *Glomus* sp. and *Alternaria* sp., high sediment kurtosis and skewness values and relatively low values with minor variations for concentration related magnetic parameters and S-Ratio (Prasad et al., 2014a). At around 1770 cal yr B.P. (Figs. 3, 6, 7), an abrupt increase in the mean grain size, sand percentage, and S-Ratio values with a peak of Zr is observed accompanied by the reappearance of *Botryococcus* alga (Fig. 4). All these parameters provide evidence for high freshwater influx, high sediment input (coarse grained MD) derived from eroded soils corresponding to a flash flood and subsequent drying and shallowing of the lake (Bøe et al., 2006; Basavaiah et al., 2010). High magnitude floods are reported at 1.7 ± 0.7 ka from the slackwater deposit records of the Mahi River (Sridhar, 2007a; Fig. 10) and in the Narmada River basin (Raj and Yadav, 2009; Sridhar et al., 2015) suggesting a regional imprint of these events.

During phase III (1730–880 cal yr B.P.) the lake levels were fluctuating under variable monsoon conditions as indicated by increase in the brown degraded palynofacies component and fungal remains, presence of *Glomus* sp., *Tetraploa* sp. and *Alternaria* sp. and higher amount of high coercivity magnetic minerals. Prasad et al. (2014a) inferred fluctuating monsoon conditions during this phase based on the pollen and phytolith data from the Wadhwana Lake. Further, the increase in sand content as compared to silt and clay and high skewness values during this phase may be attributed to lower lake levels and terrestrial admixture in the lake sediments (Liu et al., 2016). The magnetic concentration parameters and S-Ratio show fluctuating values supported by similar fluctuations in the Ba/Sr ratio suggesting a varying fluvial input during this phase. The decrease in charcoal particles (Fig. 4) and the absence of woody degraded brown material suggests reduction in biomass and shift towards dry climatic conditions and shallow lake with well-oxygenated conditions.

Similar sediment character and magnetic parameters continue during the succeeding phase IV however, marginal increase in the lake level due to higher periods of monsoon activity is suggested during this phase based on the higher percentage of degraded brown and structured OM (Prasad et al., 2014a) and lowering of the fungal remains (Quamar, 2015). The marginal increase in Thecamoebians and filamentous algae suggests existence of pristine water with good oxygenation conditions during this phase till 360 cal yr B.P.

During the phase V (0–360 cal yr B.P.) markedly finer sediments with higher magnetic mineral concentrations and mineralogical compositions were deposited as reflected in higher χ, ARM, SIRM, χfd%, SIRM/χ, Soft IRM and HIRM followed by lower S-ratio and higher Fe, Ti and Zn contents (Figs. 6 and 7). Potentially mixed origins of magnetic minerals in sediments is suggested which may have an anthropogenic, natural or mixed source (Basavaiah, 2011). Lower Ba/Sr ratio also indicates low humidity conditions.

The degraded brown phytoclasts show high presence of herbaceous remains and very low shrubs and woody fragments. Similar are the observations for the black oxidized charcoal components which primarily consist of herbs and extremely low woody fragments suggesting moderate monsoon conditions but not tenable for flourishing of the woody forested biomass (Thakur et al., 2019). The moderate to high percent of filamentous algae indicates very low water levels and formation of soil or clay rich in organic matter and lake water nutrients. Further the abundance of filamentous algae points towards enhanced human activity and eutrophication in the lake.

5.2. Comparison with regional flood events and southwest monsoon variability

The results of the present study provide evidence for two periods of river flooding in the Timbi Lake sediments. The chronology of sediments suggests that the first one occurred around 4800 cal yr B.P. and another between 2730 and 1730 cal yr B.P. however, both had distinct flooding patterns suggesting varying south west monsoon intensity. The variability in the south west monsoon conditions during the late

Holocene has been recorded from marine and continental archives of western India (Gupta et al., 2003; Kale and Baker, 2006; Chauhan et al., 2009; Sinha et al., 2007; Prasad et al., 2014a; Raj et al., 2015; Saravanan et al., 2019).

The summer monsoon precipitation decreased for around 200 years between 4200 and 4000 cal yr B.P. often known as the 4.2 ka event (Staubwasser et al., 2003; Berkelhammer et al., 2012; Dixit et al., 2014; Prasad et al., 2014b; Dixit et al., 2018). On the contrary, recent studies on the eastern Arabian Sea records suggest that weakening of south west monsoon occurred during 4600–3000 cal yr B.P. (Saravanan et al., 2019) and the lake records from western India indicate a widespread phase of aridity and drying of the lakes beginning ~5500 cal yr B.P. until ~3500 cal yr B.P. (Bryson and Swain, 1981; Singh et al., 1990; Prasad et al., 2014a, 2014b; Raj et al., 2015). The results from the Timbi lake also suggest dry climatic conditions ~4800 cal yr B.P. and occurrence of three high magnitude flood events during this period, the bottom event has been dated to 4835 cal yr B.P. Clustering of flood events during arid climatic periods and at transition from humid to arid climatic conditions has been recorded in the alluvial rivers of western India (Sridhar and Chamyal, 2018). Further, slackwater deposits in the adjacent Mahi River basin indicate flood events around 4.6 ± 1 ka (Sridhar, 2007a) and may be correlated to the flooding events in the Timbi Lake.

The records from south eastern continental margin of the Arabian Sea indicate a wet phase between 3000 and 2200 cal yr B.P. followed by century-scale climatic instabilities between 2200 and 1800 cal kyr B.P. (Chauhan et al., 2009). The period ~3200–1300 cal yr B.P. has been inferred as more or less present-day climatic pattern with fluctuating SW monsoonal activity (Fig. 10) over the Gujarat alluvial plains (Prasad et al., 2014a). Also, high southwest monsoon precipitation has been envisaged at 2800, 1110, during 600–1200 cal yr B.P. and Little Ice Age (LIA) from the Arabian Sea sediment record (Tiwari et al., 2006; Gupta et al., 2003; Anderson et al., 2002). Based on the present study, we envisage a period of multiple flood events (broadly six in number) between 2730 cal yr B.P. and 1730 cal yr B.P.; each flood event followed by a period of relatively low hydrological activity corroborating with the regional climatic variations. A high magnitude flood event at 1770 cal yr B.P. identified in the Timbi Lake probably links with coeval event recorded in the Mahi River basin (Sridhar, 2007). The sediment record at Timbi lake does not show any imprints of flooding events post 1730 cal ka B.P. as suggested by the palynological, magnetic and grain size data. However, fluctuations in the climatic conditions can be discerned and imply a shift to dry climatic conditions and fluctuating lake levels with well-oxygenated conditions till ~880 cal yr B.P., moderate increase in the lake levels till ~360 cal yr B.P. and later eutrophication of the lake. A weaker monsoon during the Little Ice Age (LIA 550–100 yr B.P.) and a relatively stronger monsoon during the Medieval Warm Period (MWP-1050–650 yr B.P.) have been envisaged from the high-resolution proxy records of Indian Summer Monsoon variability (Gupta et al., 2003; Sinha et al., 2007) which further substantiates our inference from the Timbi lake. High precipitation and wet climatic conditions during the MWP and drier conditions during the LIA have also been inferred from the lower reaches of the Narmada River based on the denudation rates of basaltic catchment (Sridhar et al., 2016).

6. Conclusions

A multiproxy study from the Timbi Lake was useful in understanding the flood pattern and its impact on sediment deposition processes during late Holocene. This lacustrine sediment sequence in the semiarid alluvial plains has provided an archive for high magnitude late Holocene river floods as well as palaeomonsoon changes. The high magnitude flood events were represented by layers of larger mean grain size and poor sorting attributed to smaller catchment and limited post-deposition reworking during the widespread phase of aridity in western India.

Relatively high quantity of coarse (MD) detrital magnetic minerals (S-Ratio, Soft IRM and HIRM) in flood event layers of the Timbi lake sediments were attributed to high discharge, vegetation changes, poor soil development and enhanced erosion. Low magnetic mineral concentration (χ, ARM and SIRM) was related to decreasing hydrological activity of the catchment area and the deposition of authigenic fine grained magnetic minerals (ARM/SIRM and χfd%) and organic-rich sediments (black oxidized and degraded brown matter and fungal remains). Peaks in S-Ratio and lows in χfd% (Fig. 9) were associated with flood pulses between 4860 and 4810 cal yr B.P. in concurrence with the onset of dry climatic conditions in the region around 5000 cal yr B.P. resulting in large sediment influx. Furthermore, desiccation-induced low vegetation cover in the catchment area, as indicated by the low representation of moist habitats (oxidized land plant tissue and black inorganic matter), might also have encouraged the sedimentation of eroded material to the lake deposits. Prolonged phase of aridity caused a depositional hiatus and sedimentation under closed environment initiated with fluctuating lake levels and reduced terrestrial influx between 2730 and 1730 cal yr B.P. as seen in the dominance of *Glomus* sp. and *Alternaria* sp. and relatively low and fluctuating values of concentration related magnetic parameters and S-Ratio. This corresponded to low magnitude high frequency floods in the catchment leading to alternate flood and non-flood layers. Enhanced monsoon conditions caused high lake levels, sediment erosion and discharge from the catchment between 880 and 360 cal yr B.P. Reduction in lake level post 360 cal yr B.P. due to sediment infill, soil formation and eutrophication of lake was inferred.

The Timbi Lake palaeoflood archive corroborates with the fluvial archive indicating a role of regional hydrological changes in response to the south west monsoon variability. High magnitude events with a low frequency were recorded during arid periods and low magnitude higher frequency events during relatively strengthened monsoon. These observations have implications for linking the palaeoflood events to the southwest monsoon intensity in the semi-arid continental regions.

Supplementary data to this article can be found online at https://doi.org/10.1016/j.palaeo.2019.109581.

Acknowledgements

This study is a part of the project DST/WOS-A/EA-1017/2015 funded by the Department of Science and Technology, India to Alpa Sridhar. We are thankful to the reviewers for their critical and constructive comments which helped in improving the manuscript. The assistance by Mr. Pranab Boral and Mr. P. Ashok, students at the Indian Institute of Geomagnetism, Navi Mumbai and Ms. Shweta Jani, student at The M. S. University of Baroda is thankfully acknowledged.

Appendix 1. Classification of palynofacies components used for the present study (after Tyson, 1995; Batten, 1996)

Groups	Subgroups/nomenclature	Composition	Origin	Characters
Phytoclasts	Structured organic matter (SOM)	Wood	Higher plants	Dark orange to brown in coloured particle from wood tracheids with or without visible pits.
		Cuticle	Land plants	Epidermal tissue of plants of cellular cells with or without stomata.
		Bark	Higher plants	Brown to dark orange coloured multicellular layered tissue
		Other tissues	Land plants	Fibrous and featureless membranous tissues
		Fungal hyphae	Fungi	Fungal mycelium of their vegetative phase
	Degraded organic matter	Degraded organic matter	Land plants	Intermediate product of plant tissue degradation with and without clear cellular margins in the same organic particle.
	Opaque phytoclasts/black oxidized OM	Charcoal and other black phytoclast	Lignin-cellulose of land plant tissues	Black particles of wood without any internal biostructure
Palynomorphs		Spores	Bryophytic or Pteridophytic	Triangular to circular palynomorphs with trilete or monolete marks; varied ornamentation
		Pollen grains	Higher plants	Varied morphology from simpler to complex: saccate to non-saccate, different type of apertures; varied ornamentation.
		Fungal spores	Fungi	Dark coloured small septate to non-septate spores, porate or non-porate
		Algal spores	Algae	Mostly pale yellow in colour, thin walled and inaperturate
Zooclasts			Faunal derivatives	Teeth, bones, hairs etc. with variable morphology and structure
Amorphous organic matter (AOM)			Degraded product of microbial activity of terrestrial origin	Structureless material with greyish or brownish in colour, homogenous, with diffused outline
Non-pollen palynomorphs (NPP)	*Botryococcus*	Algae	Flourish in freshwater lakes, ponds and temporary pools. Lacustrine environment. Indicator of hydrological changes (freshwater input)	Colonial green alga with densely packed conical–cylindrical cells radiating and branching from the centre of the roughly spherical colony
	Glomus	Fungal spore	Freshwater with erosional aspects around the area	Chlamydospores variable in size, exclusive of hyphal attachment
	Alternaria	Fungal spore	Common saprophytes found on many kinds of plants	Multicellular with both transverse and longitudinal septa, obclavate to elliptical or ovoid and provided with apical appendages.
	Tetraploa	Fungal spore	Aquatic fungi	Four vertical and a horizontal wall dividing the spore body into eight cells with four septate setae, oblong ornamented, generally with four setose and septate appendages

Appendix 2. The suite of rock magnetic parameters measured, and ratios between them that yielded information about concentration, grain size and composition of magnetic minerals and their environmental significance (Basavaiah and Khadkikar, 2004; Basavaiah, 2011; Basavaiah et al., 2018, 2019)

Parameter	Description	Reported environmental associations
Magnetic concentration parameters		
Magnetic susceptibility, χ (normalized to mass) (10^{-7} m^3/kg)	Measured as the ratio of volume susceptibility (k) to density $\chi = k/\rho$ Concentration of magnetic minerals, but is often roughly proportional to the concentration of strongly magnetic (e.g. magnetite-like) minerals. Weakly magnetic minerals, like hematite, have much lower χ values; water, organic matter have negative χ	χ is indicative of magnetizability of sediments differentiated by weathering and pedogenic processes. High values of χ represent catchment erosion inputs of primary Fe-Ti oxides from the Deccan Trap basalts of the catchment or unweathered inorganic material as a result of soil disturbance due to land-use
Anhysteretic remnant magnetization, ARM ($10^{-5}Am^2kg^{-1}$) or Anhysteretic susceptibility, χ_{ARM} (m^3/kg)	Magnetic remanence imparted in a peak 100 mT demagnetizing alternating field. When normalized by the biasing field strength, ARM is termed as the χ_{ARM}	Allows estimation of the concentration of fine-grained stable single-domain (SSD 0.025 µm < d < 0.05 µm) ferrimagnetic (magnetite-like) minerals and highest for grains at superparamagnetic (SP)/SSD boundary and lowest for coarser multidomain (MD) grains (d > 10 µm in magnetite)
Saturation isothermal remanent magnetization SIRM ($10^{-5}Am^2kg^{-1}$)	Maximum obtainable IRM, depends on concentration but also responds less sensitively than ARM to magnetic grain size	Concentration of all remanence holding minerals in a sample
Domain state		
Coefficient of frequency-dependency susceptibility χfd (%)	Variation in χ between low frequency (χlf 0.976 kHz) and high frequency (χhf 15.616 kHz) measurements $\chi fd\% = 100\ (\chi lf - \chi hf)\ /\ \chi lf$ Indicator for proportion of ultra-fine SP grains	~10% or 5–10% would indicate large fine-grained, secondary SP magnetic minerals (magnetite-like) that are the result of either weathering or pedogenesis
ARM/SIRM	Relative grain size of magnetite	High values suggest finer SSD and SP grains whereas low values indicate coarser MD minerals of detrital origin
ARM/χ	SSD and SP ferrimagnetic grains can affect the ratio	High values suggest significant SSD (magnetite-like) grains
SIRM/χ	Could distinguish different types of magnetic behaviour	Lower ratio suggests a greater proportion of diamagnetic and paramagnetic minerals. If χ and SIRM values are low, but SIRM/χ is high, there may be a large amount of hematite-like minerals
Mineralogical composition		
Isothermal remnant magnetization IRM (10^{-5} Am^2 kg^{-1})	Acquired in different DC forward and back fields	Abundance of minerals capable of remanence acquisition at the denoted field: (i) low fields (< 100 mT) magnetically 'soft' material and (ii) high fields (> 300 mT) magnetically 'hard' material
Soft IRM (SIRM–$IRM_{-0.02T}$)	Remanent magnetization after a magnetization in the 20 mT reverse field	Mass specific indication of ferrimagnetic minerals (magnetite-like) and used as a proxy to MD ferrimagnetic minerals of detrital origin
Hard IRM (HIRM) (SIRM–$IRM_{-0.3T}$)	Difference between SIRM and IRM measured after magnetization in the 300 mT reverse field	Mass specific indication of the concentration of high coercivity minerals (hematite-like), whereas 'hard' is a measure of the relative

		abundance of high coercivity (hematite-like) minerals in a mixture with ferrimagnetic (magnetite-like) minerals
S-Ratio = $IRM_{-0.3T}$ / SIRM	Ratio of saturated to non-saturated minerals at the −300 mT reverse field. Indicator for coercivity, depends on mineralogy, to a lesser degree on grain size	Higher values close to 1 are dominated by soft ferrimagnetic minerals (magnetite and titanomagnetite) with a low coercive force and lower values below 0.9 reflect increasing hard antiferromagnetic component (hematite) with a relatively high coercive force

References

Achyuthan, H., Kar, A., Eastoe, C.J., 2007. Late Quaternary-Holocene lake-level changes in the eastern margin of the Thar Desert, India. J. Paleolimnol. 38, 493–507.

Aggarwal, N., Carvalho, M., Jha, N., Thakur, B., 2017. Palynology and palynofacies of the Permian strata in the Kothagudem Subbasin, Andhra Pradesh, Southern India. J. Palaeontol. Soc. Ind. 62 (2), 175–186.

Anderson, D.M., Overpeck, J.T., Gupta, A.K., 2002. Increase in the Asian Southwest Monsoon during the past four centuries. Science 29, 596–599.

Anderson, D.M., Baulcomb, C.K., Duvivier, A.K., Gupta, A.K., 2010. Indian summer monsoon during the last two millennia. J. Quat. Sci. 25, 911–917.

Atta-Peters, D., Agama1, C.I., Asiedu, D.K., Apesegah, E., 2013. Palynology, palynofacies and palaeoenvironments of sedimentary organic matter from Bonyere – 1 Well, Tano basin, western Ghana. Int. Lett. Natural Sci. 5, 27–45.

Baker, V.R., 1987. Palaeoflood hydrology and extraordinary flood events. J. Hydrol. 96, 79–99.

Basavaiah, N., 2011. Geomagnetism-solid Earth and Upper Atmosphere Perspectives. Springer, Netherlands.

Basavaiah, N., Khadkikar, A., 2004. Environmental Magnetism and its application towards Palaeomonsoon Reconstruction. J. Indian Geophys. Uni. 8, 1–14.

Basavaiah, N., Juyal, N., Pant, R.K., Yadava, M.G., Singhvi, A.K., Appel, A., 2004. Late Quaternary climatic changes reconstructed from mineral magnetic studies from proglacial lake deposits of Higher Central Himalaya. J. Indian Geophys. Uni. 8 (1), 27–37.

Basavaiah, N., Appel, E., Lakshmi, B.V., Deenadayalan, K., Satyanarayana, K.V.V., Misra, S., Juyal, N., Malik, M.A., 2010. Revised magnetostratigraphy and nature of the fluvio-lacustrine sedimentation of the Kashmir basin, India, during Pliocene-Pleistocene. J. Geophys. Res. 115, B08105.

Basavaiah, N., Mahesh Babu, J.L.V., Gawali, P.B., Naga Kumar, K.C., Demudu, G., Prizomwala, S.P., Hanamgond, P.T., Nageswara Rao, K., 2015. Late Quaternary environmental and sea level changes from Kolleru Lake, SE India: inferences from mineral magnetic, geochemical and textural analyses. Quat. Int. 371, 197–208.

Basavaiah, N., Satyanarayana, K.V.V., Deenadayalan, K., Prasad, J.N., 2018. Does Deccan Volcanic Sequence contain more reversals than the three-Chron N-R-N flow magnetostratigraphy? - a paleomagnetic evidence from the dyke-swarm near Mumbai. Geophys. J. Int. 213, 1503–1523.

Basavaiah, N., Deenadayalan, K., Mahesh Babu, J.L.V., Kanu, M.O., Naga Kumar, K.Ch.V., Demudu, G., Nageswara Rao, K., Mallikarjunarao, N., 2019. Last 3,000 years of geomagnetic field intensity from India: New reference palaeointensity data from two east coast archaeological sites and archaeomagnetic dating insights. J. Archaeol. Sci.: Reports 27, 101943.

Batten, D.J., 1996. Palynofacies and paleoenvironmental interpretation. In: Jansonius, J., McGregor, D.C. (Eds.), Palynology: Principles and Applications. 3. American Association of Stratigraphic Palynologists Foundation, pp. 1011–1064.

Berkelhammer, M., Sinha, A., Stott, L., Cheng, H., Pausata, F.S.R., Yoshimura, K., 2012. An abrupt shift in the Indian monsoon 4000 years ago. In: Giosan, L., Fuller, D.Q., Nicoll, K., Rowan, K.F., Clift, P. (Eds.), Climates, Landscapes and Civilizations. Geophysical Monograph 198 AGU, Washington, DC.

Bierman, P., Lini, A., Zehfuss, P., Church, A., Davis, P.T., Southon, J., 1997. Postglacial ponds and alluvial fans: Records of Holocene Landscape history. GSA Today 7, 1–8.

Bird, W.B., Lei, Y., Perello, M., Polissar, P.J., Yao, T., Finney, B., Bain, D., Pompeani, D., Thompson, L.G., 2016. Late-Holocene Indian summer monsoon variability revealed from a 3300-year-long lake sediment record from Nir'pa Co, southeastern Tibet. The Holocene 1–12. https://doi.org/10.1177/0959683616670220.

Blott, S.J., Pye, K., 2001. GRADISTAT: a grain size distribution and statistics package for the analysis of unconsolidated sediments. Earth Surf. Proc. Landf. 26, 1237–1248.

Bøe, A.G., Dahl, S.O., Lie, Ø., Nesje, A., 2006. Holocene river floods in the upper Glomma catchment, southern Norway: a high-resolution multiproxy record from lacustrine sediments. The Holocene 16, 445–455.

Bronk Ramsey, C., 2001. Development of the radiocarbon calibration program. Radiocarbon 43, 355–363.

Bronk Ramsey, C., 2008. Deposition models for chronological records. Quat. Sci. Rev. 27, 42–60.

Bronk Ramsey, C., 2017. Methods for summarizing radiocarbon datasets. Radiocarbon 59, 1809–1833.

Bronstert, A., 2003. Floods and climate change: interactions and impacts. Risk Anal. 23, 545–557.

Brown, S.L., Bierman, P.R., Lini, A., Davis, P.T., Southon, J., 2002. Reconstructing lake and drainage basin history using terrestrial sediment layers: analysis of cores from a post-glacial lake in New England, USA. J. Palaeolimn. 28, 219–236.

Bryson, R.A., Swain, A.M., 1981. Holocene variations of monsoon rainfall in Rajasthan. Quarter. Res. 16, 135–145.

Cadigan, R.A., 1961. Geologic interpretation of grain-size distribution measurements of Colorado Plateau sedimentary rocks. J. Geol. 69, 121–144.

Campbell, C., 1998. Late Holocene lake sedimentology and climate change in Southern Alberta, Canada. Quarter. Res. 49, 96–101.

Carvalho, M.A., Ramos, R.R.C., Crud, M.B., Witovisk, L., Kellner, A.W.A., Silva, H.P., Grillo, O.N., Riff, D., Romano, P.S.R., 2013. Palynofacies as indicators of paleoenvironmental changes in a Cretaceous succession from the Larsen Basin, James Ross Island, Antarctica. Sediment. Geol. 295, 53–66.

Chauhan, O.S., Vogelsang, E., Basavaiah, N., Syed, A.K., 2009. Reconstruction of the variability of the southwest monsoon during the past 3 ka, from the continental margin of the Southeastern Arabian Sea. J. Quat. Sci. 25, 798–807.

Closas, M.C., Permanyer, A., Vila, M.J., 2005. Palynofacies distribution in a lacustrine basin. Geobios 38, 197–210.

Combaz, A., 1964. Les palynofacies. Rev. Micropaleontol. 7, 205–218.

Das, A., Krishnaswami, S., 2007. Elemental geochemistry of river sediments from the Deccan Traps, India: implications to sources of elements and their mobility during basalt-water interaction. Chem. Geol. 242, 232–254.

Demetrescu, E., 1998. The Chlorococcalean Alga Botryococcus and its significance in hydrocarbon exploration. In: Geo-Eco-Marina, 4/1999 Proc. Intern. Workshop on "Modern and Ancient Sedimentary Environments and Processes" in Moeciu, Romania, pp. 155–160.

Dixit, Y., Hodell, D.A., Sinha, R., Petrie, C.A., 2014. Abrupt weakening of the Indian summer monsoon at 8.2 kyr B.P. Earth Planet. Sci. Lett. 391, 16–23.

Dixit, Y., Hodell, D.A., Giesche, A., Tandon, S.K., Gázquez, F., Saini, H.S., Skinner, L.C., Mujtaba, S.A., Pawar, V., Singh, R.N., Petrie, C.A., 2018. Intensified summer monsoon and the urbanization of Indus Civilization in northwest India. Sci. Rep. 8 (1), 4225.

Ely, L.L., Enzel, Y., Baker, V.R., Kale, V.S., 1996. Paleoflood evidence of changes in the frequency of extreme floods on the Narmada River, central India. Geol. Soc. Am. Bull. 108, 1134–1148.

Enzel, Y., Ely, L.L., Mishra, S., Ramesh, R., Amit, R., Lazar, B., Rajaguru, S.N., Baker, V.R., Sandler, A., 1999. High-resolution Holocene environmental changes in the Thar desert, Northwestern India. Science 284, 125–128.

Folk, R.L., 1968. A review of grain-size parameters. Sedimentology 6, 73–93.

Folk, R.L., Ward, W.C., 1957. Brazos River Bar: a study in the significance of grain-size parameters. J. Sediment. Petrology 27, 3–6.

Friedman, G.M., 1961. Distinction between dune, beach and river sands from the textural characteristics. J. Sediment. Petrology 31, 514–529.

Gallet, S., Jahn, B.M., Torii, M., 1996. Geochemical characterization of the Luochuan loess-paleosol sequence, China, and paleoclimatic implications. Chem. Geol. 133, 67–88.

Gilli, A., Anselmetti, F.S., Glur, L., Wirth, S.P., 2013. Lake sediments as archives of recurrence rates and intensities of past flood events. In: Schneuwly-Bollschweiler, M. (Ed.), Dating Torrential Processes on Fans and Cones. Advances in Global Change Research 47https://doi.org/10.1007/978-94-007-4336-6 15.

Giosan, L., Clift, P.D., Macklin, M.G., Fuller, D.Q., Constantinescu, S., Durcan, J.A., Stevens, T., Duller, G.A.T., Tabrez, A.R., Gangal, K., Adhikari, R., Alizai, A., Filipe, F., Van Laningham, S., Syvitski, J.P.M., 2012. Fluvial landscapes of the Harappan civilization. PNAS 109, 1688–1694.

Grimm, E.C., 1987. CONISS: a FORTRAN 77 program for stratigraphically constrained cluster analysis by the method of incremental sum of squares. Comput. Geosci. 13, 13–35.

Grimm, E.C., 1990. PC spreadsheet and graphics software for pollen data. In: INQUA, Working Group on Data Handling Methods Newslett. 4. pp. 5–7.

Gupta, A., Kale, V., Rajaguru, S., 1999. The Narmada River, India-through space and time. In: Miller, A.J., Gupta, A.Z. (Eds.), Varieties of Fluvial Form. Wiley, Chichester, pp. 114–143.

Gupta, A.K., Anderson, D.M., Overpeck, J.T., 2003. Abrupt changes in the Asian southwest monsoon during the Holocene and their links to the North Atlantic Ocean. Nature 421, 354–357.

Guy-Ohlson, D., 1992. Botryococcus as an aid in the interpretation of palaeoenvironment and depositional processes. Rev. Palaeobot. Palynol. 71, 1–15.

Hoaen, A.W., 2000. The Use of Palynofacies Analysis in Archaeopalynology. PhD Thesis. University of Edinburgh, UK.

Jain, M., Tandon, S., Singhvi, A., Mishra, S., Bhatt, S., 2005. Quaternary alluvial stratigraphical development in a desert setting: a case study from the Luni River basin, Thar Desert of western India. In: Fluvial Sedimentology VII, pp. 349–371.

Jones, A.F., Macklin, M.G., Brewer, P.A., 2012. A geochemical record of flooding on the upper River Severn, UK, during the last 3750 years. Geomorphology 179, 89–105.

Juyal, N., Chamyal, L.S., Bhandari, S., Bhushan, R., Singhvi, A.K., 2006. Continental record of the southwest monsoon during the last 130ka: evidence from the southern margin of the Thar desert, India. Quat. Sci. Rev. 25, 2632–2650.

Kale, V.S., 1999. Long-period fluctuations in monsoon floods in the Deccan Peninsular, India. J. Geol. Soc. India 53, 5–15.

Kale, V.S., Baker, V.R., 2006. An extraordinary period of low-magnitude floods coinciding with the Little Ice Age: palaeoflood evidence from Central and Western India. Jour. Geol. Soc. of India 68, 477–483.

Kale, V.S., Mishra, S., Baker, V.R., 2003. Sedimentary records of palaeofloods in the bedrock gorges of the Tapi and Narmada rivers, central India. Curr. Sci. 84,

1072–1079.
King, J.W., Channell, J.E.T., 1991. Sedimentary magnetism, environmental magnetism, and magnetostratigraphy. Rev. Geophys. 29, 358–370.
Kuzucuoglu, C., Dorfler, W., Kunesh, S., Goupille, F., 2011. Mid- to late-Holocene climate change in central Turkey: the Tecer Lake record. The Holocene 21 (1713-188).
Leigh, D.S., 2018. Vertical accretion sand proxies of gaged floods along the upper Little Tennessee River, Blue Ridge Mountains, USA. Sedimentary Geol 364, 342–350.
Lepland, A., Stevens, R.L., 1996. Mineral magnetic and textural interpretations of sedimentation in the Skagerrak, eastern North Sea. Mar. Geol. 135, 51–64.
Li, Y., Guo, Y., Yu, G., 2013. An analysis of extreme flood events during the past 400 years at Taihu Lake, China. J. Hydrol. 500, 217–225.
Liu, X., Vanderberghe, J., An, Z., Li, Y., Jin, Z., Dong, J., Sun, Y., 2016. Grain size of Lake Qinghai sediments: implications for riverine input and Holocene monsoon variability. Palaeogeogr. Palaeoclimatol. Palaeoecol. 449, 41–51.
Mathur, P., Rao, K.L.N., Chaube, N., 1968. Tectonic framework of Cambay basin, India. Bulletin ONGC 5, 7–28.
Maurya, D.M., Raj, R., Chamyal, L.S., 2000. History of tectonic evolution of Gujarat Alluvial Plains, Western India during Quaternary: a review. J. Geol. Soc. India 55, 343–366.
Merh, S.S., Chamyal, L.S., 1997. The Quaternary Geology of Gujarat Alluvial Plains. Proc. Indian National Sci. Acad. 63, 1–98.
Mishra, P.K., Anoop, A., Schettler, G., Prasad, S., Jehangir, A., Menzel, P., Naumann, R., Yousuf, A.R., Basavaiah, N., Deenadayalan, K., Wiesner, M.G., Gaye, B., 2015. Reconstructed late Quaternary hydrological changes from Lake Tso Moriri, NW Himalaya. Quat. Inter. 371, 76–86.
Mueller, S., Veld, H., Nagy, J., Kürschner, W.M., 2014. Depositional history of the Upper Triassic Kapp Toscana Group on Svalbard, Norway, inferred from palynofacies analysis and organic geochemistry. Sedimentary Geol 310, 16–29.
Munoz, S.E., Giosan, L., Therrell, M.D., Jonathan, W.F.R., Shen, Z., Sullivan, R.M., Wilman, C., O'Donnell, M., Donnelly, J.M., 2018. Climatic control of Mississippi River flood hazard amplified by river engineering. Nature 556, 95–98. https://doi.org/10.1038/nature26145.
Nair, K.M., Padmalal, D., Kumaran, K.P.N., Sreeja, R., Srinivas, R., 2010. Late Quaternary evolution of Ashtamudi-Sasthamkotta lake systems of Kerala, south West India. J. Asian Earth Sci. 37, 361–372.
Oldfield, F., 2005. Environmental Change: Key Issues and Alternative Approaches. Cambridge University Press, UK.
Oldfield, F., 2007. Sources of fine-grained magnetic minerals in sediments: a problem revisited. The Holocene 17, 1265–1271.
Oldfield, F., Barnosky, C., Leopold, E.B., Smith, J.P., 1983. Mineral magnetic studies of lake sediments. Hydrobiologia 103, 37–44.
Oswald, W.W., Anderson, P.M., Brown, T.A., Brubaker, L.B., Hu, F.S., Lozhhkin, A.V., Tinner, W., Kaltenreider, P., 2005. Effects of sample mass and macrofossil type on radiocarbon dating of arctic and boreal lake sediments. Holocene 15, 758–767.
Page, M.J., Trustrum, N.A., Orpin, A.R., Carter, L., Gomez, B., Cochran, U., Mildenhall, D.C., Rogers, K.M., Brackley, H.L., Palmer, A.S., Northcote, L., 2010. Storm frequency and magnitude in response to Holocene climate variability, Lake Tutira, North-Eastern New Zealand. Mar. Geol. 270, 30–44.
Phartiyal, B., Sharma, A., Upadhyay, R., Sinha, A.K., 2005. Quaternary geology, tectonics and distribution of palaeo-and present fluvio/glacio lacustrine deposits in Ladakh, NW Indian Himalaya-a study based on field observations. Geomorphology 65 (3), 241–256.
Pocknall, D.T., Beggs, J.M., 1990. Palynofacies as a tool for the interpretation of depositional environments in the Waikato and Taranaki Basins, New Zealand. In: Proceedings of the 1989 New Zealand Oil Exploration Conference. Petroleum and Geothermal Unit, Ministry of Commerce, Wellington (NZ) (250-258 pp.).
Powell, A.J., Dodge, J.D., Lewis, J., 1990. Late Neogene to Pleistocene palynological facies of Peruvian continental margin upwelling, Leg 112. In: Suess, E., Von Huene, R. (Eds.), Proceedings of the Ocean Drilling Project, Scientific Results. 112. pp. 297–321 College Station, Texas.
Prasad, S., Enzel, Y., 2006. Holocene palaeoclimates of India. Quat. Res. 66, 442–453.
Prasad, V., Farooqui, A., Sharma, A., Phartiyal, B., Chakraborty, S., Bhandari, S., Raj, R., Singh, A., 2014a. Mid–late Holocene monsoonal variations from mainland Gujarat, India: a multiproxy study for evaluating climate culture relationship. Palaeogeogr. Palaeoclimatol. Palaeoecol. 397, 38–51.
Prasad, S., Anoop, A., Riedel, N., Sarkar, S., Menzel, P., Basavaiah, N., Krishnan, R., Fuller, D., Plessen, B., Gaye, B., Rohl, U., Wilkes, H., Sachse, D., Sawant, R., Wiesner, M.G., Stebich, M., 2014b. Prolonged monsoon droughts and links to Indo-Pacific warm pool: a Holocene record from Lonar Lake, central India. Earth Planet. Sci. Lett. 391, 171–182.
Prasad, S., Kusumgar, S., Gupta, S.K., 1997. Mid to Late Holocene record of palaeoclimatic changes from Nal Sarovar: A palaeodesert margin lake in Western India. Journal of Quaternary Science 12, 153–159.
Quamar, M.F., 2015. Non-pollen palynomorphs from the late Quaternary sediments of southwestern Madhya Pradesh (India) and their palaeoenvironmental implications. Hist. Biol. 27, 1070–1078.
Raj, R., 2004. Fluvial response to late Quaternary tectonic changes in the Dhadhar River basin, mainland Gujarat. J. Geol. Soc. India 64, 666–676.
Raj, R., Yadav, M.G., 2009. Late Holocene uplift in the lower Narmada basin, western India. Curr. Sci. 96, 985–988.
Raj, R., Chamyal, L.S., Prasad, V., Sharma, A., Thakur, B., Verma, P., 2015. Holocene climatic fluctuations in the Gujarat Alluvial Plains based on a multiproxy study of the Pariyaj Lake archive, western India. Palaeogeogr. Palaeoclimatol. Palaeoecol. 42, 60–74.
Reimer, P.J., Bard, E., Bayliss, A., Beck, J.W., Blackwell, P.G., Bronk Ramsey, C., Buck, C.E., Cheng, H., Edwards, R.L., Friedrich, M., Grootes, P.M., Guilderson, T.P., Haflidason, H., Hajdas, I., Hatte, C., Heaton, T.J., Hoffmann, D.L., Hogg, A.G., Hughen, K.A., Kaiser, K.F., Kromer, B., Manning, S.W., Niu, M., Reimer, R.W., Richards, D.A., Scott, E.M., Southon, J.R., Staff, R.A., Turney, C.S.M., van der Plicht, J., 2013. IntCal13 and MARINE13 radiocarbon age calibration curves 0–50,000 years cal B.P. Radiocarbon 55 (4), 1869–1887.
Reinwarth, B., Franz, S., Baade, J., Haberzettl, T., Kasper, T., Daut, G., Helmschrot, J., Kirsten, K.L., Quick, L.J., Meadows, M.E., Mäusbacher, R., 2013. A 700-year record on the effects of climate and human impact on the southern Cape coast inferred from lake sediments of Eilandvlei, Wilderness Embayment, South Africa. Geogr. Ann. Ser. A Phys. Geogr. 95, 345–360.
Revel-Rolland, M., Arnaud, F., Chapron, F., Desmet, M., Givelet, N., Alibert, C., McCulloch, M., 2005. Sr and Nd isotopes as tracers of clastic sources in Lake Le Bourget sediment (NW Alps, France) during the Little Ice Age: palaeohydrology implications. Chem. Geol. 224, 183–200.
Roncaglia, L., 2004. Palynofacies analysis and organic-walled dinoflagellate cysts as indicators of palaeo-hydrographic changes: an example from Holocene sediments in Skalafjord, Faroe Islands. Mar. Micropaleontology 50, 21–42.
Sandgren, P., Snowball, I., 2001. Application of mineral magnetic techniques to paleolimnology. In: Last, W.M., Smol, J.P. (Eds.), Tracking Environmental Change Using Lake Sediments. Physical and Geochemical Methods. 2. Kluwer Acad, Dordrecht, Netherlands, pp. 217–238.
Saravanan, P., Gupta, A.K., Zheng, H., Panigrahi, M.K., Prakasam, M., 2019. Late Holocene long arid phase in the Indian subcontinent as seen in shallow sediments of the eastern Arabian Sea. J. Asian Earth Sci. 181, 103915.
Schillereff, D.N., Chiverrell, R.C., Macdonald, N., Hooke, J.M., 2014. Flood stratigraphies in lake sediments: a review. Earth-Sci. Rev. 135, 17–37.
Schlolaut, G., Brauer, A., Marshall, M.H., Nakagawa, T., Staff, R., Bronk Ramsey, C., Lamb, H.F., Bryant, C.L., Naumann, R., Dulski, P., Brock, F., Yokoyama, Y., Tada, R., Haraguchi, T., 2014. Event layers in the Japanese Lake Suigetsu "SG06" sediment core: description, interpretation and climatic implications. Quat. Sci. Rev. 83, 157–170.
Sebag, D., Copard, Y., Di-Giovanni, C., Durand, A., Laignel, B., Ogier, S., Lallier-Verges, E., 2006. Palynofacies as useful tool to study origins and transfers of particulate organic matter in recent terrestrial environments: synopsis and prospect. Earth Sci. Rev. 79, 241–259.
Singh, G., Wasson, R.J., Agrawal, D.P., 1990. Vegetational and seasonal climatic changes since the last full glacial in the Thar Desert, north-west India. Rev. Palaeobot. Palynol. 64, 351–358.
Sinha, A., Cannariato, K.G., Stott, L.D., Cheng, H., Edwards, R.L., Yadava, M.G., Ramesh, R., Singh, I.B., 2007. A 900-year (600 to 1500 AD) record of the Indian summer monsoon precipitation from the core monsoon zone of India. Geophys. Res. Lett. 34, L16707.
Sridhar, A., 2007a. A mid-late Holocene flood record from the alluvial reach of the Mahi River, Western India. Catena 70, 330–339.
Sridhar, A., 2007b. Mid-late Holocene hydrological changes in the Mahi River, arid western India. Geomorphology 88, 285–297.
Sridhar, A., Chamyal, L.S., 2018. Implications of palaeohydrological proxies on late Holocene Indian Summer Monsoon variability, western India. Quat. Int. 479, 25–33.
Sridhar, A., Chamyal, L.S., Patel, M., 2014. Palaeoflood record of high-magnitude events during historical time in the Sabarmati River, Gujarat. Curr. Sci. 107, 675–679.
Sridhar, A., Laskar, A., Prasad, V., Sharma, A., Tripathi, J.K., Balaji, D., Maurya, D.M., Chamyal, L.S., 2015. Late Holocene flooding history of a tropical river in western India in response to southwest monsoon fluctuations: a multi proxy study from lower Narmada valley. Quat. Int. 371, 181–190.
Sridhar, A., Bhushan, R., Balaji, D., Band, S., Chamyal, L.S., 2016. Geochemical and Sr-Nd isotopic variations in palaeoflood deposits at mainstem - tributary junction, western India: implications on late Holocene flood events. Catena 139, 32–43.
Staubwasser, M., Sirocko, F., Grootes, P.M., Segl, M., 2003. Climate change at the 4.2 ka B termination of the Indus valley civilization and Holocene south Asian monsoon variability. Geophys. Res. Lett. 30. https://doi.org/10.1029/2002GL016822.
Thakur, B., Seth, P., Sharma, A., Pokharia, A.K., Spate, M., Farooqui, S., 2019. Linking past cultural developments to palaeoenvironmental changes from 5000 BP to present: a climate-culture reconstruction from Harshad estuary, Saurashtra, Gujarat, India. Quat.Int. 507, 188–196.
Thompson, R., Oldfield, F., 1986. Environmental Magnetism. Allen and Unwin, London, UK.
Tiwari, M., Ramesh, R., Bhushan, R., Somayajulu, B.L.K., Jull, A.J.T., Burr, G.S., 2006. Paleoproductivity variations in the equatorial Arabian Sea: implications for eastAfrican and Indian summer rainfalls and the El Niño frequency. Radiocarbon 48, 17–29.
Toonen, W.H.J., Winkel, T.G., Cohen, K.M., Prins, M.A., Middlekoop, H., 2015. Lower Rhine historical flood magnitudes of the last 450 years reproduced from grain-size measurements of flood deposits using End Member Modelling. Catena 130, 69–81.
Traverse, A., 1994. Sedimentation of Organic Particles. Cambridge University Press, pp. 557.
Tunno, I., Scott, A.M., 2017. The value of non-pollen palynomorphs in interpreting paleoecological change in the Great Basin (Nevada, USA). Quat. Res. 87, 529–543.
Tyson, R.V., 1995. Sedimentary organic matter. In: Organic Facies and Palynofacies. Chapman and Hall, London.
Tyson, R.V., Follows, B., 2000. Palynofacies prediction of distance from sediment source: a case study from the Upper cretaceous of the Pyrenees. Geol 28, 569–571.
van Geel, B., 1978. A palaeoecological study of Holocene peat bog sections in Germany and the Netherlands based on the analysis of pollen, spores and macro and microscopic remains of fungi, algae, cormophytes and animals. Rev. Palaeobot. Palynol. 25, 1–178.
van Geel, B., Gelorini, V., Lyaruu, A., Aptroot, A., Rucina, S., Marchant, R., Sinnenghe

Damsté, J.S., Verschuren, D., 2011. Diversity and ecology of tropical fungal spores from a 25,000-year palaeoenvironmental record in southeastern of Kenya. Rev. Palaeobot. Palyno. 164, 174–190.
Wilhelm, B., Arnaud, F., Enters, D., Allignol, F., Legaz, A., Magand, O., Revillon, S., Giguet-Covex, C., Malet, E., 2012. Does global warming favour the occurrence of extreme floods in European Alps? First evidences from a NW Alps proglacial lake sediment record. Clim. Chang. 113, 563–581.
Malet, E., Pignol, C., Bard, E., Delannoy, J.J., 2013. Palaeoflood activity and climate change over the last 1400 years recorded by lake sediments in the north-west. European Alps Journal of Quaternary Science 28, 189–199.
Wilhelm, B., Sabatier, P., Arnaud, F., 2015. Is a regional flood signal reproducible from lake sediments? Sedimentology 62, 1103–1117.
Wirth, S.B., Glur, L., Gilli, A., Anselmetti, F.S., 2013. Holocene flood frequency across the Central Alps-solar forcing and evidence for variations in North Atlantic atmospheric circulation. Quat. Sci. Rev. 80, 112–128.
Zobaa, M.K., Francisca, E., Oboh-Ikuenobe, Ibrahim, M.I., 2011. The Cenomanian/Turonian oceanic anoxic event in the Razzak Field, north Western Desert, Egypt: source rock potential and paleoenvironmental association. Mar. Petroleum Geol. 28, 1475–1482.